Near equiatomic FeCo alloys: constitution, mechanical and magnetic properties.

T. Sourmail

Department of Materials Science and Metallurgy, University of Cambridge

Pembroke Street, Cambridge CB2 3QZ, U.K.

email:ts228@cus.cam.ac.uk

Prog. Mater. Sci., in press, downloaded from www.thomas-sourmail.org

Abstract

Alloys based on the near-equiatomic FeCo offer exceptional magnetic properties. The equiatomic alloy was 'invented' in 1929, it offers a saturation hardly lower than that of the maximum obtained for Fe-0.35Co, with higher permeability and a lower coercivity than the latter. However, this alloy remained without industrial application, mainly because of its extreme brittleness. Only with the addition of a third element did it become possible to impart sufficient ductility for cold-rolling, and develop applications as laminated products. The addition of 2 wt% vanadium (1932) led to the ubiquitous FeCo-2V, or Permendur. It not only imparts, given appropriate heat-treatments, sufficient ductility, but also increases significantly the resistivity of the alloy while having little impact on the saturation.

From a scientific point of view, the FeCo alloys, with their B2 structure below 730 °C, fall in the interesting category of ordered compounds. The ordering reaction has significant influence on the mechanical and magnetic properties and has therefore prompted a number of investigations. Not surprisingly, the vast majority of the work published to date concerns the FeCo-2V or its variants, rather than the binary alloy or other ternary systems. Recently though, alternative compositions, or improvement on the basic FeCo-2V have been put forward.

This review attempts to summarise the current knowledge about the constitution, mechanical and magnetic properties of these alloys, focussing on the general properties of bulk FeCo and FeCo-X alloys (developped for applications such as rotor or stator laminations in motors). Recent developement of nanocomposite and

nanocrystalline materials such as HITPERM are not considered. A review of this developements is available in reference [1]. An overview is given of work undertaken to date on various FeCo-X ternary system, with emphasis on the influence of these ternary additions on microstructure and characteristics of the phase diagram. The problem of the kinetics of ordering is given particular attention. Magnetic and mechanical properties are then discussed with emphasis on the relationship between microstructure and properties, and the main quantitative theories put forward are assessed again data gathered from the literature. It is shown that, while some points are clearly understood, a number of question remains in different areas which are outlined.
Keywords: iron-cobalt alloys; soft magnetic materials, Hiperco, Permendur

Contents

1 Introduction

Iron-cobalt based alloys exhibit particularly interesting magnetic properties, with high Curie temperatures, the highest saturation magnetisations, high permeability, low losses and are relatively strong. These alloys are expensive, so are, since their discovery by Elmen in 1929 [2], confined to applications where a small volume and high performances were critical. The 'invention' of the FeCo-2V alloy in 1932 by White and Wahl [3] was a critical step in achieving an alloy of industrial relevance. Since then and despite much research, few new compositions have emerged. This is because all solute additions tend to reduce the saturation of the alloy and in general increase its coercivity, thereby degrading its magnetic performances.

There has been a resurgence of interest in these alloys, particularly in the context of the more electric engine [4], which poses a challenge for existing magnetic materials. It is envisaged, in the more electric engine concept, that there will be a greater use of embedded electrical generators and electro-magnetic bearings. To date however, a number of aspects of the FeCo-X system also remain elusive, most remarkably perhaps the role of vanadium in improving the ductility of the equiatomic alloy.

As is true for most metallic materials, a good understanding of magnetic or mechanical properties often requires a knowledge of the microstructure. This review therefore covers the microstructural aspects of FeCo alloys, attempting to sum up the knowledge available to date and identifying areas where further work is required. Because of the particular attention the ordering reaction (b.c.c. to B2 structure) has received in the literature, an entire section has been entirely dedicated to its study, detailing the methods of investigation, the influence of ternary additions of heat-treatment and of cold-work. The first section deals with the microstructure of the different alloys which have been investigated to date, that is, essentially, the transition from b.c.c. (body centred cubic) at low temperature to f.c.c. (face centred cubic) at high temperature, and the precipitation phenomena. The last section concerns the strength and ductility of these alloys, many aspects of which remain without clear explanations. Finally, a short overview is given of the most recent areas of interest.

Most of the literature refers to equiatomic alloys as 'FeCo', sometimes not specifying the exact composition which can however be off stoichiometry by one or two

percent. The units are also frequently omitted when describing a Fe-50%Co, this is of little consequence given the similar atomic masses of Fe and Co but nevertheless introduces an uncertainty of similar amplitude (equiatomic being Fe-51.3Co wt%). In the following, the compositions have been detailed whenever possible.

2 Constitution of FeCo and FeCo-X alloys

As discussed below, near-equiatomic FeCo alloys are b.c.c. at low temperature and f.c.c. at temperature above ~ 983 °C. The b.c.c. phase orders to a B2 structure at temperatures below ~ 730 °C. In a first part, the main constituents of the different FeCo based alloys are discussed; the ordering reaction is dealt with separately in the next section.

2.1 Thermodynamics of the FeCo system

Phase equilibria in the Fe-Co system are somewhat out of the scope of this review which is mainly concerned with equiatomic (or close to) compositions. It seems nevertheless useful to give a brief reminder of the phase diagram (figure 1).

Equiatomic FeCo alloys have a b.c.c structure (α in figure 1) below ~ 983 °C, with a lattice parameter given by [6]:

$$\begin{aligned} a_\alpha/\text{nm} &= 0.28236 + 6.4514 \times 10^{-5}[\text{at\%Fe}] \\ a_{\alpha_2}/\text{nm} &= 0.28250 + 6.4231 \times 10^{-5}[\text{at\%Fe}] \end{aligned} \quad (1)$$

and a f.c.c one (γ in figure 1) above this temperature, with a lattice parameter given by:

$$a_\gamma/\text{nm} = 0.35438 + 1.0233 \times 10^{-4}[\text{at\%Fe}] \quad (2)$$

There is confusion in the terminology used to refer to the different phases. The high-temperature f.c.c. phase has been referred to as γ, the disordered b.c.c. phase as α_1, and its ordered state as α_1'. (for example, [7]).

If FeCo or FeCoV alloys are quenched from a temperature inside the $\alpha_1 + \gamma$ region, the remaining γ undergoes a martensitic transformation to the b.c.c. phase. The latter has sometimes been referred to as α_2 [7–9].

Ashby *et al.* have instead used α_2 to refer to the ordered state of the b.c.c. phase, and α_1' for the martensite. They have further distinguished between γ_1, the

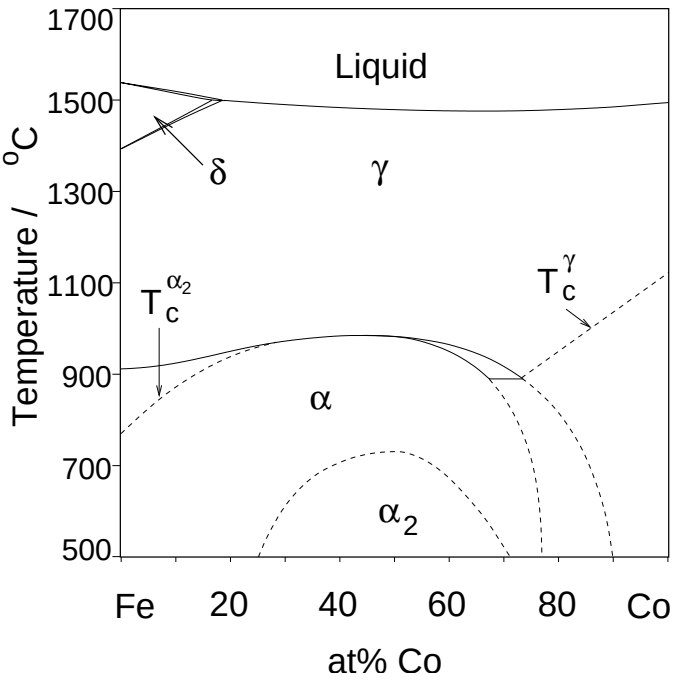

Figure 1: The Fe-Co binary diagram as given in [5]. T_c denotes the Curie temperature.

high-temperature f.c.c. phase, and γ_2, the vanadium, cobalt-rich ordered f.c.c. phase that precipitates during ageing below ~ 712 °C (in FeCo-2V, [10]). We propose to follow a similar terminology, which is consistent with that used for steels, but not stating the index 1 , *i.e.* α, α_2 (ordered), α' (martensite), γ and γ_2 (ordered f.c.c. precipitate).

The binary FeCo system has been the object of detailed studies by Ellis and Greiner (1941, [11]), Normanton *et al.* (1975, [12]) and more recently by Ohnuma *et al.* (2002, [6]) and it seems reasonable to state that there is now a good thermodynamic description of it.

A point remains obscure however, which is the so-called '550 °C anomaly' [1,13, 14] corresponding to a secondary peak in heat-capacity below that for the ordering reaction. There is much confusion even about its existence which appears to be strongly sensitive to heat-treatments and measurement conditions. It has been suggested, without further explanation, that this is a kinetic effect as it is not observed in measurements where the temperature is varied slowly enough [12,15], however recent works also have questioned this assumption [13], and in one case, even proposed that this corresponds to a phase-transition [14], as discussed in section 3.3.

2.2 The Fe-Co-V system

This section is concerned with the Fe-Co-V system in regions of interest for typical FeCo-2 alloys, *i.e.* compositions close to equiatomic FeCo with small additions of V.

In spite of the fact that the FeCo-V alloys are the only one to have been industrially produced (FeCo being too brittle), the determination of the phase diagram leaves many areas which need clarification.

2.2.1 $\alpha/\alpha+\gamma$ boundary

A number of studies have focused on the determination of the $\alpha/\alpha+\gamma$ and $\alpha+\gamma/\gamma$ boundary [7–10, 16–18]. It is undisputed that vanadium additions reduce both the $\alpha/\alpha+\gamma$ and $\alpha+\gamma/\gamma$ transition temperatures (further denoted $T_{\alpha/\alpha+\gamma}$ and $T_{\alpha+\gamma/\gamma}$).

It has emphasised [10, 19] that there exists significant discrepancy between the different estimations of these temperatures. It also appears that no further assessment of the Fe-Co-V system has been undertaken. Figure 2 illustrates the differences between the prediction obtained with the thermodynamic calculation software MTDATA [20] and different estimations of the two-phase region.

Figure 3 illustrate a similar isopleth as determined by Martin and Geisler [16], which suggests a solubility of up to 4 wt% V around 700 °C. It is also noticeable that ordering is not found past 10 wt% V, this has been also reported by Foutain and Libsch [15].

As mentioned above, there is agreement that vanadium lowers $T_{\alpha/\alpha+\gamma}$ and $T_{\alpha+\gamma/\gamma}$, but authors have emphasised the large interval of estimated values. However, it appears that the exact stoichiometry has sometimes been neglected in comparisons. For example, while some of the values obtained by Martin and Geisler [16], or Ashby *et al.* [10] are for equiatomic content in Fe and Co, other values are for alloys with identical wt% of Fe and Co, which corresponds to an excess of Fe in at% (for example, Bennett and Pinnel, [7]).

Figure 4 superimposes results from a number of studies, and shows that there is reasonable agreement between the values obtained by Martin and Geisler [16] by thermal analysis (lines), and the phases identified by Ashby *et al.* [10] in materials quenched from high-temperature after 24 h heat-treatment, in equiatomic FeCo-2V. However, data obtained from alloys with excess Fe (empty symbols in figure 4) seem

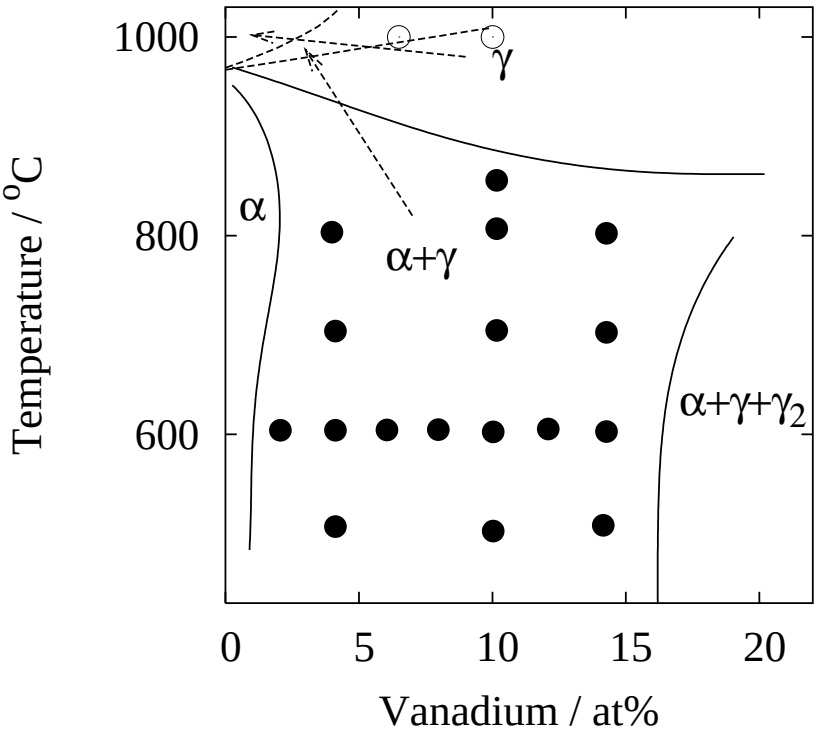

Figure 2: Isopleth section at 52 at% Co for the FeCoV system. Dotted lines indicate the calculation made using MT-DATA and the SGTE solution database, solid lines and data point are from Koster *et al.* [21, 22]; ∘ are points identified as single-phased regions and • as two-phases regions.

to indicate higher values for $T_{\alpha/\alpha+\gamma}$ and $T_{\alpha+\gamma/\gamma}$, while values for alloys with Co excess (crossed symbols in 4) seem to lie lower than those estimated for equiatomic alloys. From this, it could be proposed that, in composition with excess Fe (empty symbols), vanadium does not depress $T_{\alpha/\alpha+\gamma}$ and $T_{\alpha+\gamma/\gamma}$ as strongly, while it is more efficient in alloys with excess Co.

This may not be the case, though, as the results obtained by Kawahara [23] who reports $T_{\alpha/\alpha+\gamma}$=882 °C and $T_{\alpha+\gamma/\gamma}$=945 °C (averaging values measured during heating and cooling) for an alloy with 51Fe-47Co-2V (at%), are in excellent agreement with the results from Martin and Geisler [16] despite the off-stoichiometric composition.

It has been mentioned above the the γ phase may transform to martensite upon quenching to room temperature. The morphology of the martensite has been reported with a varyingly pronounced lath-like morphology [8, 10]. While Mahajan

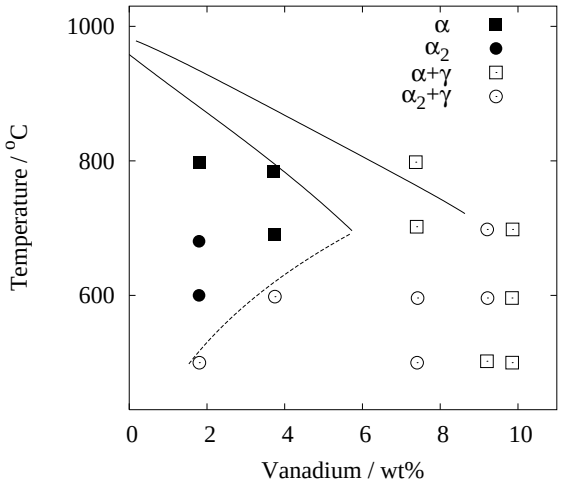

Figure 3: Isopleth section at 52% Co in FeCo-V system, after Martin and Geisler [16]. Solid lines indicate boundaries determined by thermal analyses, phases are otherwise identified by X-ray diffraction.

et al. [8] suggest that this might be the result of the transformation being partially massive, partially martensitic, Ashby *et al.* [10] proposed that this is essentially dependent on the vanadium content of the prior γ phase: the higher the V-content, the lower the martensite start (M_s) temperature, and the more pronounced is the lath shape.

Additions of vanadium are also reported to lower the ordering temperature (713 °C for FeCo with 2 wt% V [24]).

2.2.2 Lower temperature phases

There is significant confusion over the phase-diagram at lower temperature. As illustrated in figure 2, Koster and Schmidt (1955, [21, 22]) propose that γ is found in FeCo alloys with more than 1-2 at% V (it should however be noted that the diagram is not a section through equiatomic FeCo, as wrongly quoted by Chen [17], and that a 2% V addition corresponds to 46Fe-52Co-2V). This section also leaves significant uncertainty about the exact position of the $\alpha/\alpha + \gamma$ boundary at low vanadium content, and proposes that the ordered f.c.c. γ_2 phase only exists at higher vanadium content.

Further investigations, however, do not necessarily support the diagram proposed

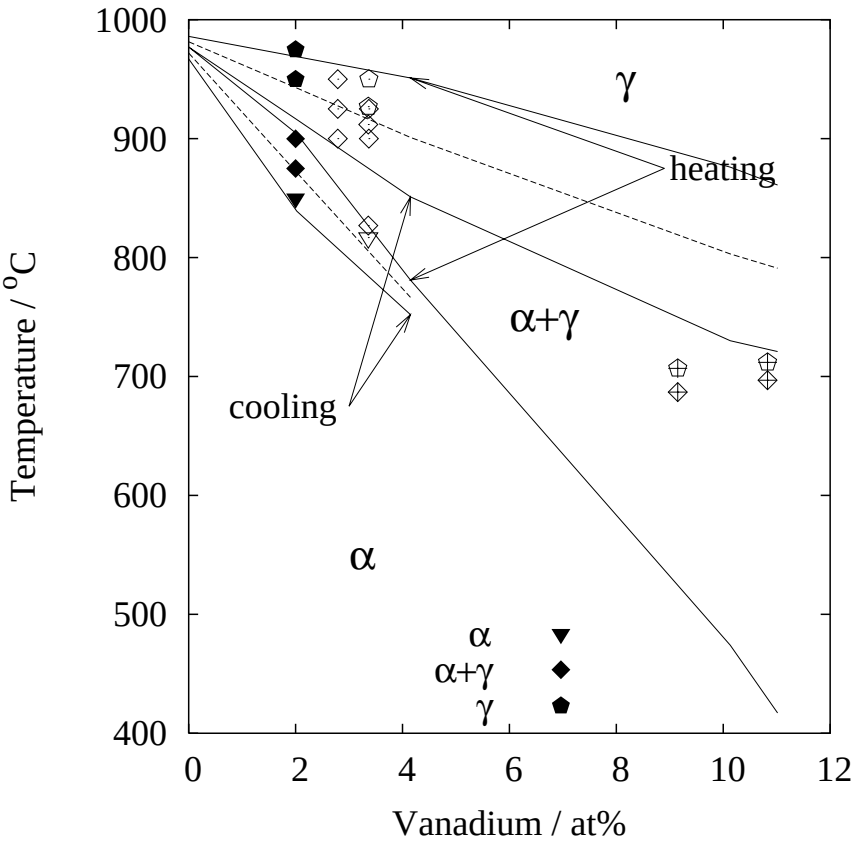

Figure 4: The $\alpha/\alpha+\gamma$ and $\alpha+\gamma/\gamma$ boundaries as a function of vanadium content in an equiatomic FeCo alloy, as measured by Martin and Geisler [16] by thermal analysis (lines, dotted lines are average of values measured during cooling and heating), and comparison with other published data [7, 10, 16]. Filled points represent values for equiatomic compositions, empty points indicate alloys with excess Fe (addition of V at the expense of Co) and crossed points indicate alloys with excess Co (addition of V at the expense of Fe).

by Koster and Schmidt, in particular with regard to the formation of γ at lower temperatures. For example, Chen (1961, [17]) did not confirm the formation of γ phase, after 110 h at 565 °C, for a FeCo-2V alloy (it must be noted however that many experimental details remain unclarified). Fiedler and Davis (1970, [25]) later reported precipitation of γ in a cold-rolled FeCo-2V after 48 h at 680 °C, and noted that this precipitation was not observed in a sample first recrystallised at higher temperature. They also estimated the composition of the precipitate phase to 22V-65Co-15Fe (wt%). Bennett and Pinnel (1974, [7]) noted the inconsistency between

the composition proposed in [25] and the isotherm section of Fe-Co-V proposed by Koster and Schmidt [21], which places the γ formed at low temperature in the $\alpha + \gamma + \gamma_2$ field. However, the problem remained discussed in terms of $\alpha + \gamma$ equilibrium (for example [8, 26]) until the work of Ashby *et al.* (1976, [10]), who proposed that the phase precipitating at low temperature is not γ but a Fe-substituted variant of the Co_3V compound, $(Fe,Co)_3V$, with $L1_2$ structure (ordered f.c.c.), vanadium occupying the corner of the lattice and (though not stated) Fe and Co mixing on the face centres.

Although they observed the forbidden reflections {001} and {110} in electron diffraction, they were unable to do so using X-ray diffraction and argued that this was a consequence of the very similar X-ray scattering factor of Fe and Co. This argument is frequently put forward to explain the low intensity of the superlattice reflections of ordered b.c.c FeCo, but it is not clear how it would apply here: if one assumes a random distribution of Co and Fe on the face centres and, with Ashby *et al.*, vanadium on the cube corners, the {110} reflection, for example, relates to $[(0.83 f_{\mathrm{Co}} + 0.17 f_{\mathrm{Fe}}) - f_{\mathrm{V}}] \sim (f_{\mathrm{Fe}} - f_{\mathrm{V}})$, and it is therefore the similar scattering factor of Fe,Co and V which explain the difficulty in observing the superlattice peaks (the atomic scattering factor of V is intermediate between Fe and Co, leading to an even smaller difference than in of ordered b.c.c. FeCo so that the conclusion remains valid).

The ordered γ_2 phase has also been reported by Pitt and Rawlings (1981, [18]) in Fe-Co-V-Ni, however there is no explanation of how the $L1_2$ structure was identified.

Further investigations have usually accepted the hypothesis of a $L1_2$ structure for γ_2 (or that γ_2 was the compound $(Fe,Co)_3V$ rather than a prolongation of the high-temperature γ phase), for example [19, 23, 27, 28], although it appears that none have obtained independent confirmation of the structure. The composition proposed by Fiedler and Davis [25] was confirmed by Kawahara (1983, [23]) who reported 21V-64Co-15Fe (wt%) for γ_2.

Surprisingly, in a recent investigation on the ageing (200 h at 450 °C) of FeCo-2V, Zhu *et al.* [29] report the formation of a primitive cubic second phase, of lattice parameter 2.8278 Å, and although refer to past literature on γ_2, do not comment on the discrepancy with the otherwise accepted structure.

In summary, although it seems accepted that the vanadium rich phase precipitating out of α FeCo-2V below $\sim$ 630 °C is an iron-substituted form of Co_3V, with

an ordered $L1_2$ structure, there have been no attempts to correct the FeCo-V phase diagram proposed by Koster and Schmidt. The ordered nature of the precipitate has been reported in only one work, and most other observations are based on the composition being close to that expected from such a compound.

Kinetics of precipitation The kinetics of precipitation of γ_2 have been studied by Ashby *et al.* [10] for FeCo-2V and Pitt and Rawlings [18] for the same alloy with additions of Ni up to 7.4 wt%.

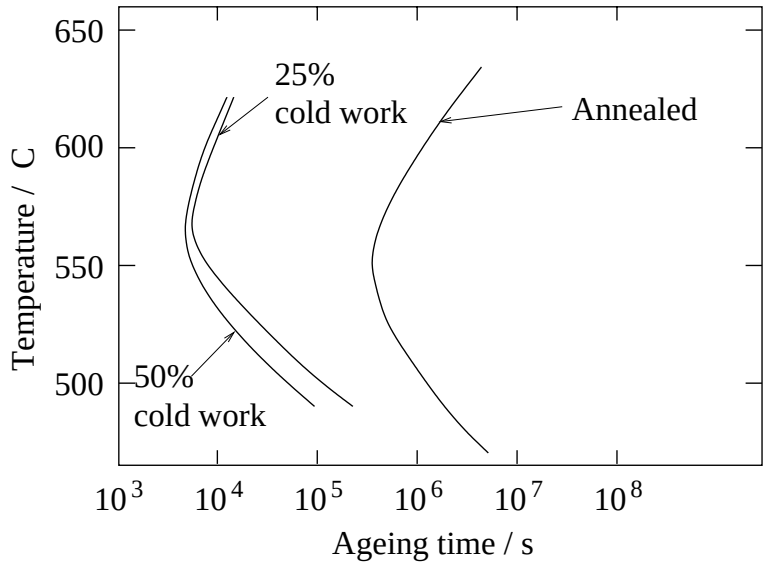

Figure 5: TTP diagram for intragranular γ_2 formation in FeCo-2%V, after Ashby *et al.* [10].

After verifying that a 10 ks heat-treatment at 850 °C produced a fully α microstructure, Ashby *et al.* aged undeformed, 25% and 50% cold-rolled samples. Their results are summarised in a TTP (time temperature precipitation) diagram reproduced in figure 5. Precipitation occurs preferentially on antiphase boundaries in the undeformed samples; it is accelerated by deformation, γ_2 being found mainly on dislocations and subgrain boundaries in cold-rolled samples. The TTP diagram does not include high-angle grain boundary precipitates which are found at early stages of ageing in all samples.

The time required to observe γ_2 on the grain boundaries is not clear in the work of Ashby *et al.*; a study by Novotny [30] underlines the absence of any γ_2 after 4 h

at 845 °C followed by cooling at 100 °C/h, suggesting that grain boundary γ_2 does not occur fast enough to be observed after slow cooling.

A number of studies provide measurements of precipitates volume fraction. Yu *et al.* [31] reported diameter and volume fraction of precipitates in FeCo-2V and FeCo-2V-0.3Nb during ageing at 600 °C (figure 6).

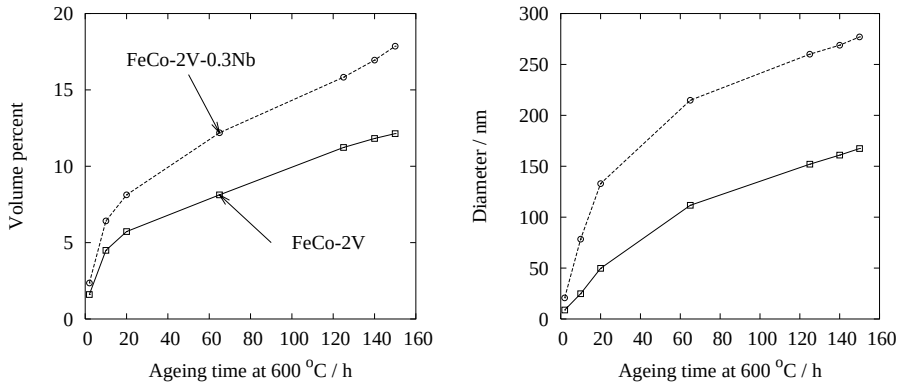

Figure 6: Volume percent and diameter of precipitates during ageing of FeCo-2V and FeCo-2V-0.3Nb according to Yu *et al.* [31].

Although the problem of determining the volume fraction of small particles is notoriously difficult, and require assumptions as to their shape and distribution, the work published in [31] does not provide any detail about the experimental methods used. The measured composition of γ_2 (about 18V at%) means a maximum mole fraction of about 10% if the solubility of vanadium is taken to be 0 (α and γ_2 having similar molar volume, mole fractions are used in this discussion, but it is expected that volume fraction would be very similar), or 5% if a more realistic assumption of 1% solubility is assumed. Large volume fraction of γ_2 have been reported by different authors [24, 28], but in alloys containing up to 6V at%; it was verified that these were consistent with the maximum expected from the composition. The large inconsistency between estimated maximum ($\sim 5\%$) and measured volume fractions ($12-18\%$) in Yu *et al.*'s study [31] cast some doubts on the validity of these results, all the more that the authors claim to have confirmed a $(FeCo)_3M$ type formula for the precipitates.

Unfortunately, although a number of studies report volume fractions of γ_2 after short annealing treatments [18, 32], there does not appear to be data other than those discussed above for aged samples.

Results by Zhu *et al.* [29] suggest the presence of a vanadium-rich phase in 0.3% volume fraction in FeCo-2V, increasing to 0.8% after 200 h at 450 °C. However, they report a simple cubic structure with a lattice parameter of 2.8278 Å, while γ_2 is usually accepted that γ_2 is an ordered LI_2 structure of lattice parameter 3.56 Å.

2.2.3 Influence of quaternary additions

Nickel additions Pitt and Rawling [18] have investigated the influence of Ni additions to a FeCo-2%V, varying the Ni content from 0 to 7.4 wt%. The results of their investigations show that nickel stabilises γ_2. This implies that larger amounts are obtained (about 7% of γ_2 after 2 h at 750 °C for nickel contents between 3.5 and 7.4 wt%. The kinetics are also affected, with times to detect precipitation an order of magnitude smaller with additions of 3.5% Ni and more. The authors suggests that nickel substitute for Fe or Co in the compound $(Fe,Co)_3V$, however not providing evidence of its ordered nature, nor of its exact composition, which is only reported to be vanadium and nickel rich. There are a number of problems with these results:

- the authors report, that, for any amount of nickel between 3.5 and 7.4 wt%, the amounts of second-phase are very similar. This is surprising given that one of these alloys has a vanadium content half of the others (0.7 wt%).
- the volume fractions reported sometimes exceed the theoretical maximum (for zero vanadium solubility) and in all cases suggest a very low solubility for vanadium.

It is therefore difficult, for lack of direct evidence, and support from the other observations, to accept the hypothesis of Ni substituting for Fe or Co in $(Fe,Co)_3V$. Furthermore, Orrock [19] reported precipitation of a phase of composition close to $(Fe,Co)_3Ni$ in FeCo-5Ni (at%). Such a composition would be consistent with the amount of γ_2 increasing with increasing Ni content, and with the volume fractions larger than calculated on the basis of vanadium solubility alone.

The effect of smaller quantities of nickel (< 0.7 wt%), corresponding to contamination rather than deliberate additions has been investigated by Novotny [30]. The author proposes that additions of more than 0.3 wt% Ni lead to a significant decrease of $T_{\alpha/\alpha+\gamma}$ and report the presence of martensite in high Ni sample (0.7 wt%) annealed at 885 °C and cooled at 100 K/h to room temperature.

Mention is also made of the absence of γ_2. This is not inconsistent with the results of Pitt and Rawlings who indicate no γ_2 in lower Ni alloys following slow cooling from 750 °C.

Niobium additions There does not appear to have been any systematic study of Nb additions in FeCo-V. As discussed in a later section, it has been proposed that a compound similar to γ_2 forms in FeCo-Nb the system [24, 28], however there is no clear agreement over the phases found in FeCoV-Nb. The most commonly studied alloy in this system is potentially Hiperco H50HS (Carpenter Ltd), which contains typically $\sim$ 2V and $\sim$ 0.3Nb (wt%) [31–35]; but few studies have investigated the microstructure of this alloy.

Yu *et al.* (2000, [31]) have suggested occurrence of a γ_2-type phase (figure 6), however, the problems outlined in section 2.2.2 remain, in particular for the FeCoV-Nb system in which the volume fractions reported are totally inconsistent with the suggested compositions of the precipitates. In addition, the phrasing in [31] makes it difficult to separate the findings of the authors from quoted results. Shang *et al.* (2000, [33]) have, on the other hand, reported formation of niobium carbonitrides in alloys with additions of 0.06 wt% Nb (and $\sim$ 0.01% C) and Laves-phase $(Fe,Co)_2Nb$ in alloys with 0.3 wt% Nb. This behaviour is more consistent with, for example, that of Nb in other Fe-based alloys. In austenitic stainless steels, for example, Nb forms NbC to its solubility limit, excess Nb forming Laves phase at a later stage [36]. It is not clear from the work quoted in [33] whether niobium carbides are observed together with Laves phase in materials containing excess Nb.

Other additions Orrock [19] investigated the effect of tungsten and copper additions to FeCo-V, and reported the formation of f.c.c. copper precipitates ($a = 0.3608$ nm) in an alloy with 5% Cu annealed at 760 °C. γ_2 was found in FeCo-V with 3 and 5 wt% W additions after annealing at 850 °C.

2.3 Other Fe-Co-X systems

There is data for a few other ternary systems [37–43]. However, in a number of cases, no further work appear to have been undertaken since the 30s. In most of these investigations, which concern the entire ternary system, the precision is not

sufficient to be of any use in the design of equiatomic FeCo alloys.

2.3.1 Fe-Co-Cr

Although the system has been investigated by a number of authors (for example [41, 44, 45], a review is given in [46]), data in the area of interest for high-saturation equiatomic FeCo alloys are far from accurate and mostly extrapolated or even guessed. The influence of Cr additions on $T_{\alpha/\alpha+\gamma}$ and $T_{\alpha+\gamma/\gamma}$ is illustrated in figure 7.

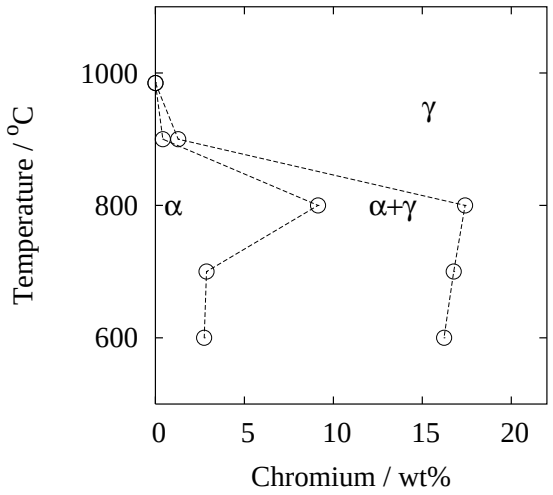

Figure 7: The influence of Cr on the $\alpha/\alpha+\gamma$ and $\alpha+\gamma/\gamma$ boundaries. Constructed from the isotherm section in [46]. These isotherms are largely extrapolated if not guessed in this region.

2.3.2 Fe-Co-Ni

Work on Fe-Co-Ni has been reviewed by Rivlin [46]. Figure 8 is a pseudo-binary diagram constructed from isothermal ternary sections published in the literature [46–48]. The phases were determined by long-term ageing at the given temperatures.

2.3.3 Fe-Co-Mn

Figure 8 shows a construction of the isopleth FeCo-Mn for equiatomic alloys, constructed from the isothermal ternary sections by Köster and Speidel [49]. The

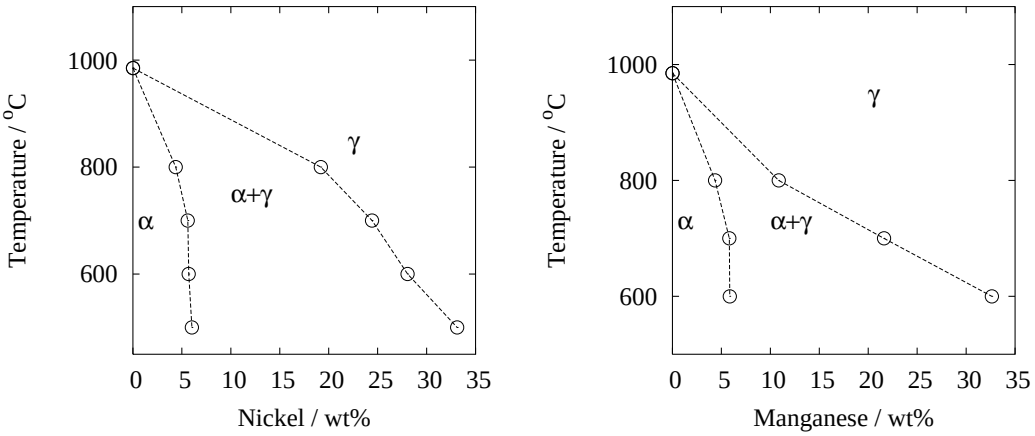

Figure 8: The influence of Ni and Mn on the $\alpha/\alpha+\gamma$ and $\alpha+\gamma/\gamma$ boundaries. FeCo-Ni constructed from the isotherm sections in [46]. FeCo-Mn from isotherm sections in [49]. It should be noted that these isotherms are largely extrapolated if not guessed in this region.

authors also reported a significant influence on T_k, which is lowered to ~ 685 °C for a 3 wt% addition of Mn.

As noted in section 5.2, Mn does not impart enough ductility to obtain a cold-workable alloy [50].

2.3.4 Fe-Co-W

The FeCo-W system has been partially studied by Köster [51] and Köster and Tonn [37], although, as mentioned earlier, there is no reliable assessment of the impact of small additions of W to equiatomic FeCo alloys. Orrock [19] report a significant influence of a 1 wt% addition on $T_{\alpha/\alpha+\gamma}$, lowered from 977 °C to about 910 °C, while further additions up to 5 wt% do not affect $T_{\alpha/\alpha+\gamma}$. As discussed in section 5.2, W addition do not, in most cases, lead to a workable alloy, which probably explain the little interest in the system.

2.3.5 Fe-Co-Nb

The FeCo-Nb system has been studied by Rezende *et al.* [52] and Persiano and Rawlings [24,28]. Nb as limited solubility in equiatomic FeCo alloys, estimated to 0.3 at% [24]. This result was obtained for samples furnace cooled from 760 or 850 °C, and it is therefore not straightforward to assess which temperature it is representative

of, particularly as there is evidence that precipitation occurs even during cooling (table 1). Beyond this limit, increasing amounts of spherical paramagnetic particles are found, of composition 49Co-35Fe-15Nb at% [24]. It must be emphasised that,

Nb / at%	FC	IBQ
0.62	7	6
1.24	11	10
1.77	14	11

Table 1: The volume fraction of second phase identified in equiatomic FeCo annealed 2 h at 850 °C and furnace cooled (FC) or quenched in iced brine (IBQ). After [24]

while the authors suggest that this may be the previously mentioned $L1_2$ structure, they do not provide evidence for the structure.

According to differential thermal analysis [24], Nb has no impact, either on $T_{\alpha/\alpha+\gamma}$ or T_k. The former (averaged over heating/cooling) appears to vary by less than 5 °C with increasing amounts of Nb (up to 1.77 at%), and there is no detectable opening of the $\alpha+\gamma$ field as is the case for V additions. T_k is constant and reported as 731 °C ±2.

2.3.6 Fe-Co-Si and Fe-Co-Al

Griest *et al.* [53] reported the effect of small Si and Al additions in FeCo alloys. In thermal analysis studies, silicon was found to raise the ordering temperature but also reduce the amplitude of the corresponding peak (for example, $T_k = 805$ °C for 2 wt% Si). It also lowered the $T_{\alpha/\alpha+\gamma}$ and $T_{\alpha+\gamma/\gamma}$ temperature, (in the vicinity of 940 °C for 2 wt% Si). Al was found to have a similar impact on T_c ($T_k = 808$ °C for 2 wt% Al), but little effect on $T_{\alpha/\alpha+\gamma}$ and $T_{\alpha+\gamma/\gamma}$.

2.4 Recrystallisation and grain-growth

As will be discussed later, many of the mechanical and magnetic properties of FeCo based alloys are conditioned by the grain size. It appeared therefore appropriate to discuss the problem of recrystallisation and grain-growth.

Because of the ordering reaction, recrystallisation and grain-growth do not follow standard behaviour. Using X-ray, Borodkina *et al.* [54] studied the recovery and

recrystallisation of FeCo alloys of different stoichiometries. Their results indicate that, while recovery is detected earliest in the equiatomic alloy, recrystallisation is slowest for this composition. In particular, remainders of the deformation texture are still present even after 1 h at 800 °C. These authors also suggest that recrystallisation does not begin below T_k, with the argument that recrystallisation below T_k implies the formation of a disordered structure, and might therefore not be thermodynamically advantageous. It is not clear why, however, one would assume that recrystallised grains must be disordered.

In further work, Seliskii and Tolochko [55] and Goldenberg and Seliskii [56] studied the same problem using optical microscopy instead of X-rays, and reported similar conclusions.

Later, Davies and Stoloff [57] studied the kinetics of recrystallisation for a FeCo-2V alloy and reported significantly different results: after similar thickness reductions (90%), complete recrystallisation occurred after 1 h at 650 °C, while Goldenberg and Seliskii suggested that recrystallisation only started after 8 h at 700 °C in a FeCo alloy. Furthermore, the grain sizes reported in both studies are vastly different. For example, Davies and Stoloff [57] report a grain size of 12 μm after 1 h at 750 °C, while, in Seliskii and Tolochko's work [55], the grain size only reaches ~ 3 μm after 8 h at 750 °C. This is illustrated in figure 9; the thickness reduction in [58] is not specified, but as the authors used commercial sheets provided by Carpenter Ltd, it seems reasonable to assume that these have been cold-rolled to 90% thickness reduction as usually reported.

Further studies are also contradictory with regard to the recrystallisation kinetics. Thornburg [59] reported only 10-20% recrystallisation in FeCo-2V, cold-rolled to 90% reduction in thickness and annealed 2 h at 670 °C, with full recrystallisation only achieved, at 710 °C. Similarly, Pitt and Rawlings [18] report an equiaxed, recovered structure with subgrain size of about 1 μm, for FeCo-2V after 2 h at 680 °C. This appears to be in contradiction with the results of Davies and Stoloff, who, for identical material and conditions, observed full recrystallisation after 1h at 650 °C.

One possibility is that the latter authors have mistaken the well developed subgrain structure reported by Pitt and Rawlings [18], for a recrystallised structure. In the absence of misorientation measurements, it is difficult to assess these results. Subgrain boundaries are believed to have a similar impact on strength as grain

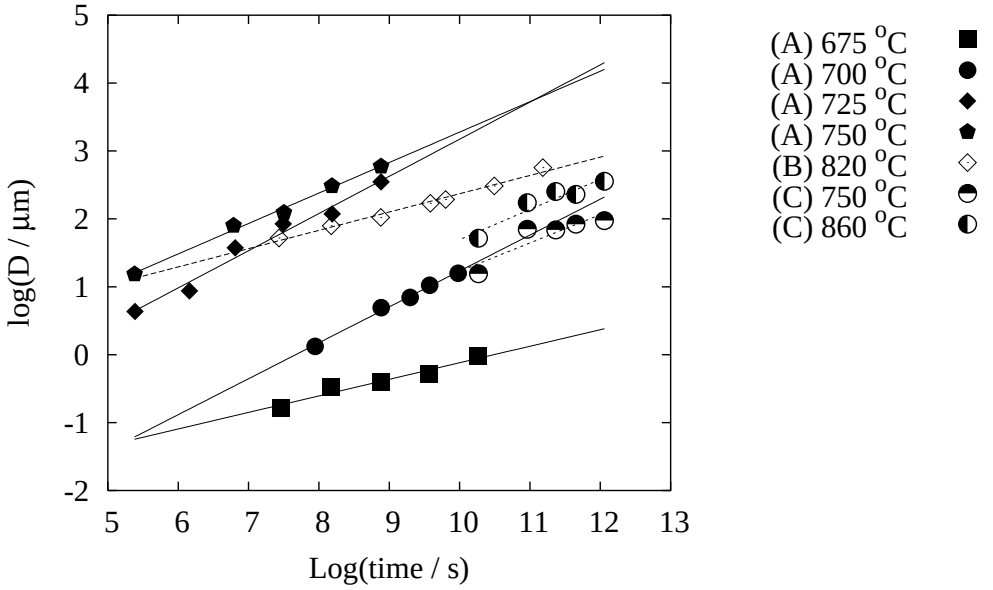

Figure 9: The grain size as a function of time during annealing at varying temperatures following deformation. (A) FeCo-2V, drawn, area reduction 75% [57], (B) FeCo-2V-.05Nb, cold-rolled, thickness reduction presumed 90% [58], (C) FeCo, cold-rolled, thickness reduction 82% [55].

boundaries, which can be modelled by an equation of the type [60] :

$$\sigma_y = \sigma_0 + cd^{-m} \tag{3}$$

Because of their low misorientation however, their impact is significantly less, that is to say, c is expected to be significantly smaller than typical values as determined for grain boundary strengthening.

Using independent published data on the grain size, the present author showed [61] that the strength measured by Thornburg [59] matched very well that expected from the grain sizes reported by Davies and Stoloff [57], implying that the strengthening effect is as expected for a normal grain structure rather than a subgrain one.

Recent developments have confirmed and exploited (for example [62]) the possibility for these alloys to recrystallise at low temperature. Buckley [63, 64] investigated the interactions between the ordering reaction and recrystallisation. Using an FeCo-0.4Cr alloy deformed to about 40%, he distinguished four temperature regions as illustrated in table 2.

The authors pointed out that, while at intermediate temperatures ($475 < T < 600$ °C), only recovery occurred even after times up to 100 h, recrystallisation was

Annealing temperature / °C	Observation
$> T_c$	recrystallisation in disordered state, rapid.
$600 < T < 725$	very fast ordering, recrystallisation slower
$475 < T < 600$	ordering, recovery
$250 < T < 475$	ordering and recrystallisation to very fine grains

Table 2: Recrystallisation and ordering in FeCo-0.4Cr, after Buckley [63].

observed at lower temperatures. He proposed that, while the ordering reaction occurs before and independently of recrystallisation at higher temperatures, the ordering proceeds, at lower ($T < 475$ °C) temperature, through the formation of new ordered grains. However, according to Buckley [63, 64], this does not seem to occur in FeCo-V alloys, where no recrystallisation is observed at lower temperatures.

Recent results from Duckham *et al.* [65] show a 70 % recrystallised structure after 5 h at 438 °C and almost 100 % after 1 h at 600 °C, for a FeCo-1.8V-0.3Nb cold-rolled to 93% reduction in thickness. These heat-treatments lead to grain-sizes of 100 and 150 nm respectively. Once again, it is not impossible that this is a misidentification of a well developed subgrain structure.

Kinetics of grain growth Davies and Stoloff (1966, [57]) studied grain growth in FeCo-2V and used a parabolic growth rate to fit their data:

$$D^2 = \sigma V K_0 \exp\left(\frac{-Q_g}{RT}\right) t \tag{4}$$

where D is the grain size, σ the grain-boundary energy per unit area, V the molar volume, K_0 the pre-exponential factor for the grain boundary mobility $K = K_0 \exp(-\Delta Q/(RT))$, Q_g the activation energy, T the temperature and t the duration of the annealing treatment. $K' = K_0 \sigma V$ will be used for further discussion. Part of their results are shown in figure 9.

These authors reported an activation energy of $Q_g \sim 238$ kJ/mol in the disordered state ($T > T_c$), and pointed out the difficulty of fitting a single value of

activation energy at lower temperature, where the ordering reaction is expected to continuously modify this value.

More recently, Yu *et al.* [58, 66] studied the grain growth kinetics of FeCo-1.9V-0.05Nb (figure 9). Despite the higher temperature, this alloy exhibits slower grain growth as expected from the addition of a small amount of Nb. It is not clear, however, as to how the authors obtained the value of $Q_g = 240.3$ kJ/mol, given that growth was characterised at only one temperature. In these conditions, obtaining Q_g implies knowledge of the pre-exponential factor K', for which the authors give no value. While it can be worked out that a value of $K' \sim 8.3 \times 10^{-4}$ m^2 s^{-1} must have been used by these authors, the only value which may have been available from the literature is $K' \sim 5.5 \times 10^{-2}$ m^2 s^{-1} [57].

In conclusion, also there is good agreement concerning the recrystallisation behaviour at high and low temperatures, there is a need for clarification regarding the evolution of deformed structures in FeCo just below T_c (650-720 °C), in particular, whether only recovery occurs around these temperatures or whether the observations can be explained by a large change in the grain growth rate in the ordered condition.

3 Ordering of Fe-Co

It is commonly accepted that Fe-Co undergoes an ordering transition around 730 °C where the b.c.c. structure takes the CsCl (B2) ordered structure (figure 10).

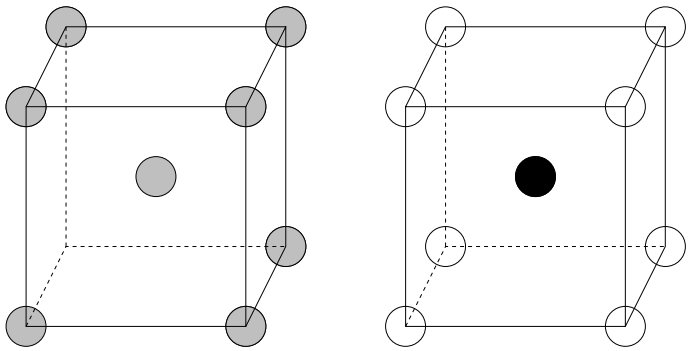

Figure 10: b.c.c. and ordered B2 structure.

Before discussing the characteristics of the ordering reaction in Fe-Co and related alloys, the experimental methods most often used in investigations of the ordering reaction are briefly presented.

The kinetics of the ordering reaction are commonly described in terms of the evolution of the long range order parameter S, defined for this structure, by $S = 2(p - \frac{1}{2})$, where p is the fraction of, say, Fe atoms occupying Fe sites. This is 0.5 for a fully disordered alloy (and therefore $S = 0$) and 1 for a fully ordered equiatomic alloy ($S = 1$).

Before presenting the results, the experimental techniques most commonly used for the estimation of the order parameter are briefly reviewed.

3.1 Experimental methods

3.1.1 Lattice parameter measurements

Bozorth (1951, [67]), measured the lattice parameter change accompanying the ordering of Fe-Co for Co varying between 0 and 80 at%. The ordering reaction only occurs between 29 and 70 at% Co [12], and causes an increase of lattice parameter, from 2.8485 to 2.8506 Å. This method has also been used by Clegg and Buckley [68], who report a 0.2% change in lattice parameter between the disordered and ordered

phases, with a change from 2.8550 to 2.8570 Å. The order parameter S is assumed to be proportional to the increase of lattice parameter.

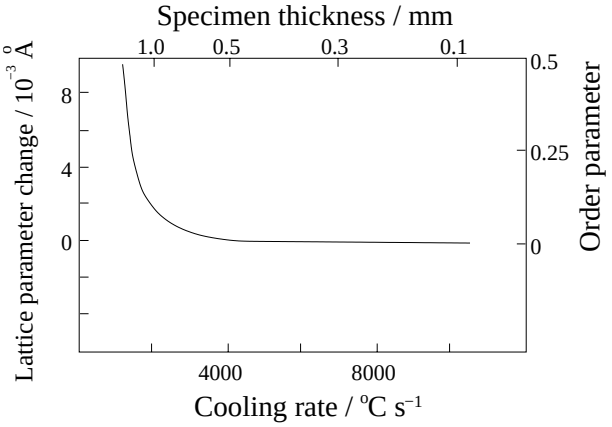

Figure 11: The lattice parameter change caused by ordering as a function of the cooling rate, in equiatomic FeCo, and FeCo-2.5V. The ordering reaction can be avoided with cooling rates greater than $\sim$ 4000 °C/s. After [68].

3.1.2 Superlattice reflections

Upon ordering, the lattice type changes to primitive and the intensity for lines otherwise forbidden in b.c.c. becomes non-zero. However, this intensity remains extremely small if conventional X-ray methods are used, because of the similar atomic factors of Fe and Co. If a wavelength near the absorption edge of one of the scattering elements is used in a diffraction experiment, anomalous scattering effects occur that can enhance the intensity of these lines by an order of magnitude [68]. Most studies have therefore made use of Co or Fe K_α radiations in X-ray experiments. The order parameter can be related to the ratio $I_{\{100\}}/I_{\{200\}}$ where $I_{\{hkl\}}$ is the intensity of the line of corresponding indices, more exactly:

$$S^2 = R\frac{I_{\{100\}}}{I_{\{200\}}} \tag{5}$$

where R includes Lorentz and polarisation factors.

Most often, this method is used to estimate $S/S_{\max}$ rather than an absolute value of S [18,63,64,68]. $S_{\max}$ refers to the value of S for a fully ordered system. Different references have been used for $S_{\max}$: although some authors have used ordered binary

FeCo for which S is close to one (and $I_{\{100\}}/I_{\{200\}} = 1/66.1$) [18], others have used the equilibrium state of the system studied (for example, [68]). In the former case, the values estimated are close to the absolute ones In the latter, and particularly in the study of ternary FeCo-X alloys, they provide an over-estimation of the order parameter, because the absolute value of the equilibrium order parameter in FeCo-X is below one.

In the case of neutron diffraction [29, 69, 70], the absolute order parameter can be obtained. In ternary FeCo-X systems, this requires assumptions as to the distribution of the X.

3.1.3 Magnetic measurement

Various methods have been used to correlate magnetic properties changes and the disorder-order transition. Measurements of the saturation moment show an increase of about 4% upon ordering [17, 68, 71, 72], as illustrated in figure 12.

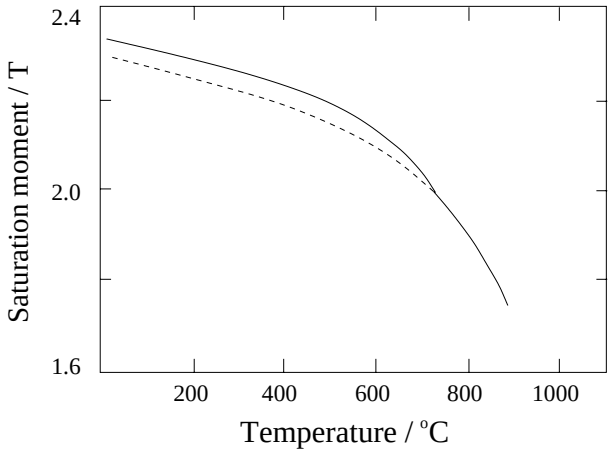

Figure 12: The variation of the saturation magnetisation as a function of temperature, after [68].

3.2 Kinetics of ordering

The kinetics of ordering of FeCo and related alloys has been the focus of much attention in the 1970s with particular emphasis on the role of vanadium additions.

3.2.1 Ordering of binary FeCo alloy

Early evidence for ordering were presented by Kussmann *et al.* [73], Rodgers and Maddocks (1939 [74]) and Shull and Siegel (1949 [70]). Ellis and Greiner [11] provided an accurate measurement of the ordering temperature for equiatomic FeCo, reporting a value of $T_k = 732$ °C, but values as low as 710 °C have also been reported [12].

The ordering reaction in equiatomic FeCo is very rapid, so that the cooling rates required to obtain fully disordered samples cannot be achieved in industrial scale processes. Clegg and Buckley [68] investigated the kinetics of the ordering reaction in equiatomic Fe-Co using lattice parameters measurement. Quenching samples of different thicknesses in iced brine (after 30 min at 810 °C), they estimated that ordering was totally avoided only for quenching rates greater than $\sim$ 4000 °C/s (figure 11). This value was estimated from the specimen thickness (700 μm).

The equilibrium degree of order depends on temperature, particularly near the critical temperature. Using X-rays, Stoloff and Davies [75] reported the long-range order parameter in FeCo-2V, as a function of temperature and showed that these measures compared well with other results obtained by different techniques, and with theoretical values. This is illustrated in figure 13. It must be noticed that variations of the order parameter occur essentially between 600 °C and T_k.

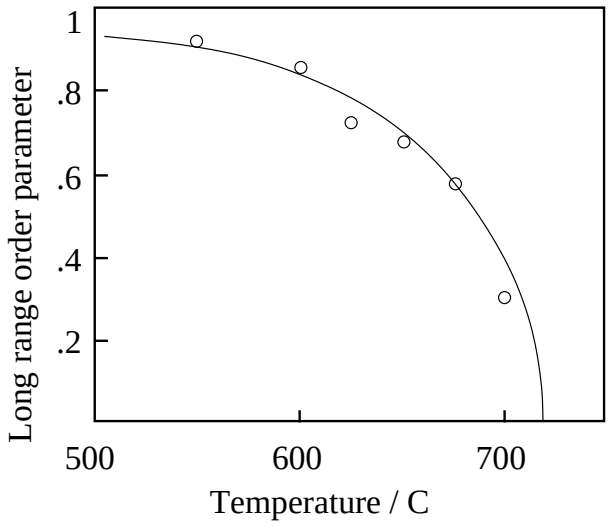

Figure 13: The long range order parameter as a function of temperature in FeCo, after [75].

An activation energy Q_o can be calculated for the kinetics of the ordering reaction, although some studies emphasise the difficulty in giving it a clear physical meaning [68, 76]. Particular difficulties arise in the physical interpretation of the ordering rates as the kinetics of quenched-in vacancies annihilation is similar, so that both phenomena must be considered together [76]. Values tend to be in reasonable agreement with each other; for example $Q_o = 188$ kJ/mol [76], or 160 kJ/mol [68]. Rajkovic and Buckley [77] report $Q_o = 105$ kJ/mol for heterogeneous ordering (see below) at low temperature.

Ordering mechanism: Clegg and Buckley [68] then Buckley [64] found two distinct ordering mechanisms in binary Fe-Co:

- Above 500 °C but to a lesser degree down to 430 °C, ordering is homogeneous, followed by antiphase domain (APD) coalescence.
- Between 260 °C and 430 °C approximately, the authors observed nucleation and growth of grain boundary films of fully ordered structure.

The kinetics of domain coalescence in binary FeCo alloys have been studied by Clegg and Buckley [68], and later Rajkovic and Buckley [77]. As mentioned above, when ordering above $\sim$ 400 °C, the process is homogeneous, in which case domains of constant size are observed while the long-range degree of order increases. Once S has reached its equilibrium value, APD coalescence begins [78]. The coalescence stage is generally well fitted to:

$$d^2 - {d_0}^2 = kt \tag{6}$$

where d is the domain size, d_0 the domain size at $t = 0$, and k is related to the antiphase boundary mobility and can be written:

$$k = k' \exp\left(-\frac{Q_d}{RT}\right) \tag{7}$$

A value of $Q_d = 264$ kJ/mol for the activation energy of the antiphase boundary mobility has been calculated by the present author from published data [77], while Grosbras *et al.* [76] report a value of 190 kJ/mol. Both studies have however investigated APD growth in the same range of temperature following similar annealing conditions. This activation energy is in general expected to be identical to that for volume diffusion in the disordered material [68], and although there is no data for the binary alloy, this has been confirmed in FeCo-2V.

3.2.2 Influence of vanadium addition

As will be shown, the agreement over the influence of vanadium additions on the kinetics of ordering remains poor after more than 50 years of investigations.

The FeCo-2V composition was first proposed by White and Wahl [3] in 1932. Through addition of about 2% vanadium and in conjunction with appropriate heat-treatment, equiatomic FeCo alloys become workable (this is further discussed in section 5.2). The ordered α_2 phase is frequently observed to be very brittle while the disordered α may have some ductility. This lead to the hypothesis that vanadium slows the ordering process and allow ductility to be retained through quenching. The absence of direct evidence was underlined by Stanley (1950 [79]).

A number of investigations followed which cast doubts on this hypothesis. In 1973, Clegg and Buckley [68] showed that the critical cooling rate to avoid ordering was similar in FeCo and FeCo-2.5V. These results were based on lattice parameter measurements (figure 11), but were validated by comparison to magnetic and X-ray diffraction data. As for FeCo, a cooling rate of about 4000 °C/s, corresponding to a thickness of 700 μm quenched in iced brine, was required to obtain a fully disordered sample. A similar limit was proposed by Smith and Rawlings in 1976 [69], who used neutron diffraction to study the kinetics of ordering in FeCo-1.8V: while a 600 μm sample quenched in iced brine from 850 °C lead to a fully disordered sample, the order parameter in the as-quenched state for a 1 mm sample was about 0.3.

Most studies have concentrated on the kinetics of ordering during reheating after quench. Clegg and Buckley (1973, [68]), then Buckley (1975, [64]), showed that, the kinetics of ordering of FeCo and FeCo-2.5V are similar over a wide range of temperatures. Some of these results are summarised in figure 20, which shows the times to reach $S/S_{\max} = 0.5$ and $S/S_{\max} = 0.95$ during isothermal annealing after quenching from 810 °C. The same authors also investigated the effect of larger vanadium contents (5.1%) and observed a retardation of the ordering reaction [68].

Subsequent studies do not completely agree with these results. Eymery *et al.* (1974, [80]), used X-rays to estimate the evolution of $S/S_{\max}$ during isothermal annealing of FeCo and FeCo-2V after quenching samples of 1 mm thickness from different temperatures. The reference used for $S_{\max}$ is unfortunately not stated As illustrated in figure 15, these authors gave evidence that the vanadium containing alloy orders faster than the binary one, although it appears that the initial degree

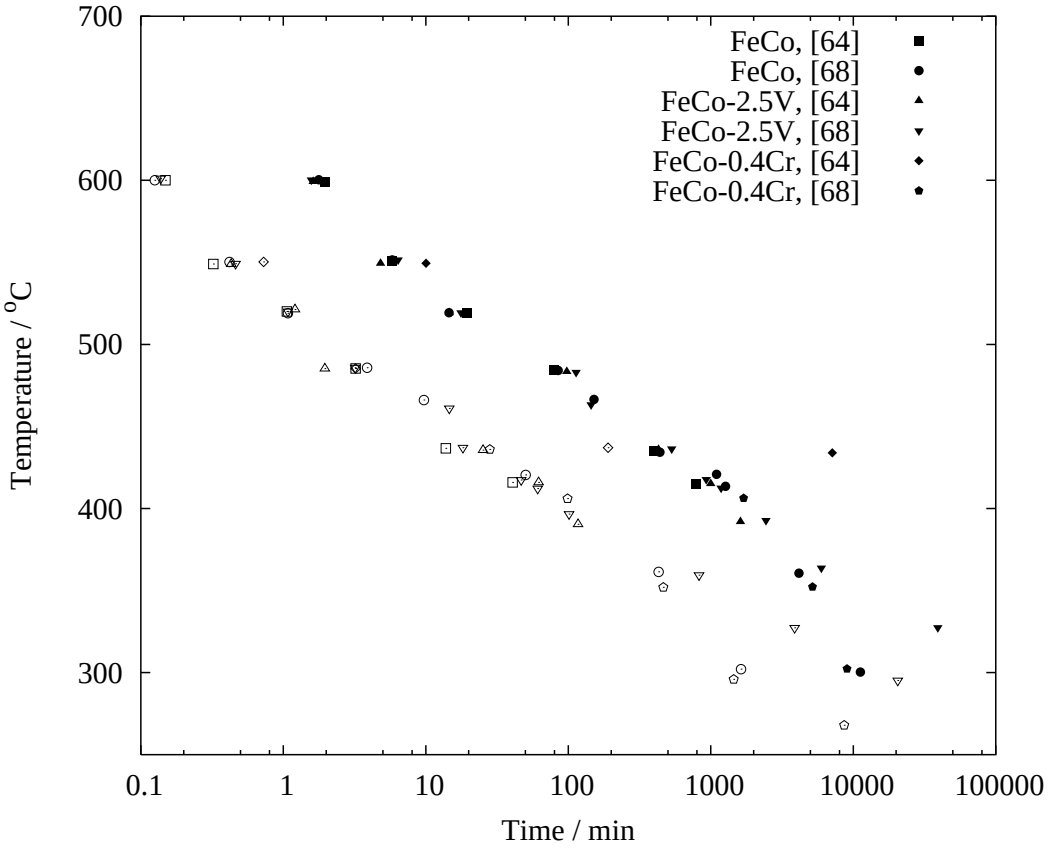

Figure 14: The times to reach S/S_{max}=0.5 (empty symbols) and S/S_{max}=0.95 (full symbols) in FeCo based alloys with different additions, after quench in iced brine from 810 °C. After [64, 68].

of order is lower in the vanadium containing alloy.

Eymery *et al.* (1974, [80]) and later Grobras *et al.* (1976, [76]) proposed that a higher concentration of quenched-in vacancies in FeCo-V than in FeCo explains the difference; this in turn would be caused by a strong interaction between vacancy and vanadium. The formation of numbers of dislocation loops and helices during low-temperature annealing was taken as evidence for this large concentration of quenched-in vacancies [76].

Measurements of ordering kinetics by Smith and Rawlings (1976, [69]) on FeCo-1.8V are consistent with previous studies, but provide a more reliable estimate of the equilibrium degree of order in this material. The value estimated from neutron diffraction, assuming distribution of V on both Fe and Co sites, was 0.80. The authors further support the hypothesis made by Grosbras *et al.* [76] on the role

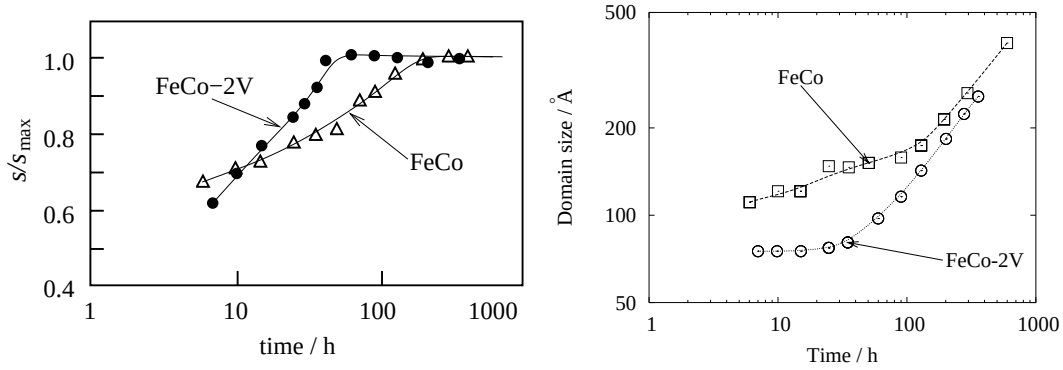

Figure 15: Isothermal ordering kinetics at 440 °C for FeCo and FeCo-2V quenched from 780 °C. After Eymery *et al.* [80]. Isothermal domain growth in same conditions, after Grobras *et al.* [76].

of quenched-in vacancies by showing that the activation energy for the ordering evolution increases towards that for diffusion as the process occurs. This can be explained by the rapid disappearance of the excess vacancies.

The results reported above are in clear contradiction with the hypothesis that vanadium slows the ordering kinetics. More recently however, results by Orrock and Major [19] and Orrock [68] provided support for this hypothesis. Using lattice parameters measurements, the authors estimated the degree of order for 2.5 mm samples of various FeCo-X alloys quenched in iced brine from 850 °C. Their results are illustrated in figure 16.

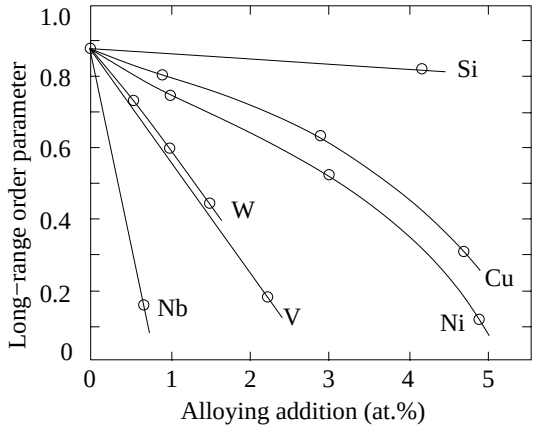

Figure 16: The ordering parameter of binary and ternary FeCo alloys as a function of elemental additions, after quenching into ice brine from 730 °C. After [19, 81].

Although a significant amount of order is to be expected from the thickness of the specimen used in Orrock's work, it is difficult to reconcile the largely different order parameters for FeCo and FeCo-2V with the previous results indicating identical ordering kinetics in these systems. To date, there does not appear to be an explanation for this paradox.

Overall, Orrock's results are the only ones supporting the early hypothesis that vanadium slows ordering and therefore helps obtain a ductile alloy. Most other results indicate no effect or even an acceleration of the ordering reaction by vanadium. It should be emphasised however that few studies [19, 68] have compared the order parameter of FeCo and FeCo-V for identical quenching conditions, most work having focused on the ordering kinetics during annealing.

Discarding the Clegg and Buckley [68] study, the results are consistent in as much as measurements by Eymery *et al.* [80] indicate a lower order parameter for FeCo-2V after quenching (figure 15). There is, however no obvious reason to doubt the work of Clegg and Buckley. Furthermore, if one were to accept that vanadium retards the ordering during quenching but not annealing, it would still be necessary to propose a mechanism explaining this paradoxical behaviour.

It seems therefore reasonable to suggest that measurements and comparisons of the order parameters for FeCo and FeCo-2V following quenching at different rates should be repeated, if possible with a direct method such as neutron diffraction. If such results were are to confirm Orrock's measurements rather than Clegg and Buckley's one, work would be required to understand the 'double' effect of vanadium on the ordering reaction.

As for the binary alloy, it is possible to estimate an activation energy for the ordering process. Values are in reasonable agreement with the exception of one study (table 3).

Q_o / kJ mol^{-1}	Reference
160	Clegg and Buckley [68]
170	Rajkovic and Buckley [77]
154	Grosbras *et al.* [76]
255	Smith and Rawlings [82]

Table 3: The activation energy for the ordering reaction in FeCo-2V alloys.

Ordering mechanism: Clegg and Buckley (1973, [68]), Buckley (1975, [64]), and Rajkovic and Buckley (1981 [77]) have investigated the ordering mechanisms in FeCo-V alloys of different compositions. As mentioned earlier, the binary alloy has been found to order homogeneously at high temperatures, but by nucleation and growth of an ordered phase at lower temperatures. With increasing vanadium additions however, the transition disappears, and the conventional FeCo-2V alloys exhibit homogeneous ordering at all temperatures. This is illustrated in figure 17.

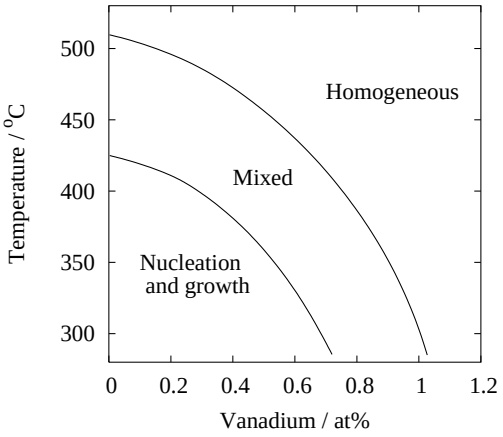

Figure 17: The ordering mechanism of FeCo-V alloys as a function of temperature and vanadium content, for samples quenched from 800 °C, after [77].

In the temperature range where mechanisms differ, the FeCo-V alloys are found to order more slowly than FeCo or, as discussed later, FeCo-Cr (figure 14).

A number of studies [68, 76, 80, 83–85] have investigated the coalescence of domains in FeCo-V during homogeneous ordering, and reported values for the activation energy as described in section 3.2.1. These include English [83] and Clegg and Buckley [68], whose methods were later criticised by Rogers *et al.* [84] who recalculated values of Q_d based on the data published by the former authors. Results are summarised in table 4 which highlights some discrepancies between different studies. Most of the results fall reasonably close to the activation energy for volume diffusion in the disordered material, estimated to 250-300 kJ/mol.

3.2.3 Influence of chromium additions

Very few studies have dealt with the influence of Cr additions to FeCo [63, 64].

Q_d / kJ.mol^{-1}	Reference
294	English [83]
337	recalculated by Rogers *et al.* [84] from data in [83]
284	Clegg and Buckley [68]
213	recalculated by Rogers *et al.* [84] from data in [68]
178	Rogers *et al.* [84]
251	Grosbras *et al.* [76] and Eymery *et al.* [80]

Table 4: The activation energy for the APD boundary mobility as estimated by various authors.

Clegg and Buckley [68] compared the kinetics of isothermal ordering of a FeCo-0.4Cr to binary FeCo and FeCo-2.5V, at 435 °C and 550 °C and observed significant retardation of the ordering reaction. However, Buckley [64] later concluded the opposite, and showed that ordering kinetics and mechanisms of FeCo-0.4Cr are the same as for the binary system (figure 14) in the temperature range 260-600 °C.

3.2.4 Influence of niobium additions

Clegg and Buckley [68] first investigated the effect of small niobium addition (0.4%). Measuring the isothermal kinetics of FeCo-0.4Nb at 435 and 550 °C, they observed a strong retardation compared to FeCo or FeCo-2V, particularly at 435 °C (more than one order of magnitude).

The impact of Nb on the ability to retain the disordered state of FeCo alloys through quenching is further supported by Major and Orrock [81]. The details of this study have been reviewed earlier (section 3.2.2). As illustrated in figure 16, Nb appears to be the most effective in helping retaining a low degree of order after quench.

In more recent studies, Persiano and Rawlings (1991, [24, 28]) have investigated the influence of higher Nb content (1, 2 and 3 wt%). Using 250 μm thick samples quenched in iced brine from 850 °C, the authors investigated the isothermal ordering kinetics at 550 °C with X-rays and showed an 0.62 at% Nb addition results in retardation by one to two order of magnitudes compared to FeCo or FeCoV as measured by Clegg and Buckley [68]. As will be discussed later, the use of a higher quenching temperature than that used by Clegg and Buckley (850 instead of 810 °C) implies

that the difference could be even larger if an identical disordering temperature is used.

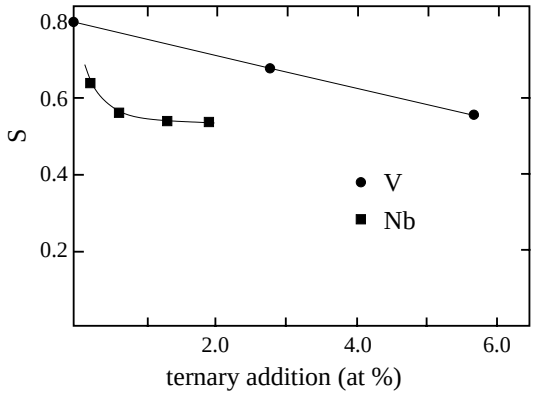

Figure 18: The equilibrium or near-equilibrium degree of order in different FeCo-X alloys, at 550 °C. After [28].

Yu *et al.* (1999, [32]) undertook direct measurement of order parameter by neutron diffraction for FeCo-2V-0.3Nb following quench at different rates from 820 °C, and obtained a negligible order parameter (0.04) for a quenching rate of 30000 °C/h, *i.e.* $\sim$ 8.3 °C/s, which is considerably less than the estimated 3000 °C/s for FeCo-2V [68].

Niobium additions not only have an impact on kinetics, but also on the maximum degree of order that can be reached, as indicated by Persiano and Rawlings [28], who report the equilibrium or near-equilibrium degree of order to be close to only 0.5 with a 2% addition of Nb; this represent a stronger impact than vanadium (figure 18).

3.2.5 Influence of other elements

Very few studies have been found that deal directly with the influence of other elements on the degree of order, although, as will be discussed later, more work has been done on the ductility of the as-quenched state, which seems closely related to the ordering phenomenon.

Orrock [19] used lattice parameter measurements to determine the degree of order in 2.5 mm think strips of various FeCo-X alloys, (and FeCo-2V-X). The results are illustrated in figure 16. Si is found to have little impact, Cu and Ni a mild impact, W and V a stronger impact and Nb the strongest one.

In the FeCo-2V-X system however, Si seems to have an opposite effect and reduce the 'quenchability' of the disordered state, while W and Cu have no effect up to about 2 and 5 at% respectively (figure 19). This shows that the combined effect of different solutes cannot easily be inferred from their individual impact.

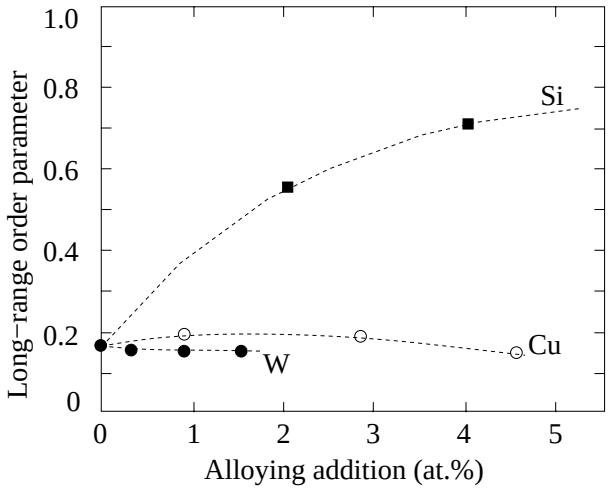

Figure 19: The variation of long-range order parameter for 2.5 mm strips of various compositions, quenched from 850 °C. After [19].

3.2.6 Influence of quenching temperature

The influence of the temperature from which the alloy is quenched before isothermal ordering has been studied by Eymery *et al.* (1974, [80]) and Smith and Rawlings (1976, [69]). It is illustrated in figure 20. The accelerated ordering kinetics for disordering temperatures in the range 730-850 °C is explained by the increase of excess vacancies quenched in the material (section 3.2.2). The discontinuity above 850 °C is attributed to entering the $\alpha + \gamma$ field.

3.2.7 Influence of cold work

Grobras *et al.* (1973, [78]), Eymery *et al.* (1974, [80]) and later Smith and Rawlings (1976, [69]) have investigated the effect of cold-work on the isothermal ordering kinetics. The former authors deformed samples at room temperature after quenching 1 mm thick FeCo-2V samples from 780 °C, then followed the evolution of the long-range order parameter by X-ray diffraction, during annealing at 440 °C. Their results

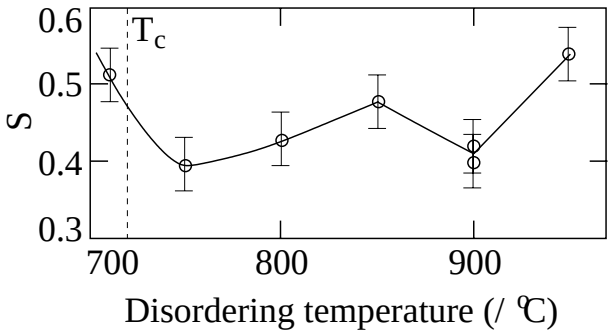

Figure 20: The degree of order achieved after 500 s at 450 °C in a 48.4Fe-49.8Co-1.8V wt%, as a function of the prior 'disordering' temperature.

indicate that for 10 or 20% thickness reduction, ordering is initially accelerated, but hindered towards the end of the reaction, reaching equilibrium order well after the non-deformed samples.

Smith and Rawlings [69] used 0.6 mm thick FeCo-1.8V samples quenched from 850 °C, deformed by cold-rolling (25-75%), then followed the ordering kinetics using neutron diffraction at 450, 475 and 500 °C. Their results indicate, on the contrary, that the reaction is slower throughout. Having observed that dislocations sub-structures consist of cells whose size is an order of magnitude larger than that of the domains at the end of the ordering reaction, they conclude that the dislocation obstacle effect can probably not account fully for the retardation. Also, there appears to be no recovery nor recrystallisation at the temperatures investigated (within the duration of the ordering reaction). They propose that the dislocations play an important role both as vacancies sinks during the ordering reaction and by reducing the short-range order (and therefore the number of ordered nuclei) during prior deformation.

An experiment can here be suggested which would provide further support for this hypothesis. A higher quenching temperature implies a higher concentration of quenched in vacancies but lower number density of ordered embryo. If the effect of deformation on the vacancy concentration is more important, the ordering kinetics after deformation, in a sample quenched from a lower temperature will be proportionally less affected than one quenched from a higher temperature. If on the other hand, after quenching from a higher temperature, deformation has less influence, then it might be supposed that the main effect is on the ordered embryos.

3.3 Challenging the existence of an ordering reaction

Although the existence of an ordering reaction, together with its implications, have been a working hypothesis for the past 50 years, recent work has challenged up to the existence of an ordered phase in bulk FeCo and emphasised the importance of the 550 °C anomaly in explaining the magnetic properties of these alloys. The problem has been reviewed in details by the present author [86]. It was found that numerous published results could not be reconciled with the new theory. In addition, some of the results put forward as evidence for this new theory could not be reproduced.

4 Magnetic and electrical properties

The following section discuss the magnetic properties of FeCo based alloys, essentially with respect to the microstructural features of the alloy.

4.1 Overview

Iron-cobalt alloys have the highest magnetisation saturation of all known magnetic alloys (figure 21).

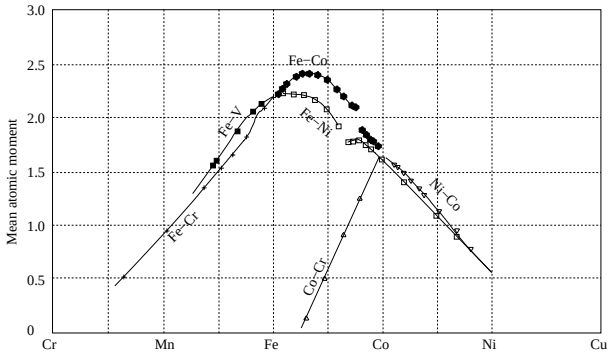

Figure 21: The Slater-Pauling curve showing the mean atomic moment for a variety of binary alloys as a function of their composition, after [67].

Although the maximum saturation is obtained around 35% cobalt, equiatomic compositions offer a considerably larger permeability for a similar saturation, as illustrated in figure 22.

As for soft magnetic systems in general, the coercivity of FeCo alloys depends strongly on the microstructure. It is out of the scope of this review to discuss the

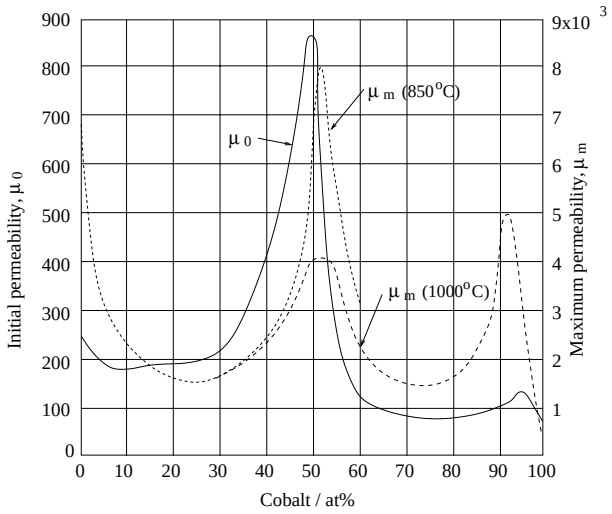

Figure 22: Initial and maximum permeability for Fe-Co alloys, the annealing temperature influences strongly the maximum permeability, in this case most likely because 1000 °C lies in the two-phase region. After [67].

theories describing this dependency, the focus being on reviewing the impact of composition and thermomechanical treatment on the magnetic properties.

4.2 The saturation of FeCo based alloys

The saturation magnetisation is generally regarded as independent of the microstructure. As indicated earlier (figure 12), an increase of saturation has been observed following ordering, which in turns has been used as an indicator of the order parameter. Although the moments of Co atoms does not depend on their environment, that of Fe does, as it increases from 2.2 μ_B in pure Fe to about 3 μ_B (figure 23) in ordered equiatomic FeCo [67, 69, 87]. This is rather spectacularly illustrated in the measurement of the saturation of FeCo alloys where a solid solution is obtained by mechanical milling of pure Fe and Co particles (figure 23).

Typical saturation values for ordered binary FeCo [72] or FeCo-2V [19, 24] are about 2.35 T.

Chen [67] investigated the influence of ternary additions on the saturation of FeCo alloys, and found that most (Ti, V, Cr, Ni, Cu) had a detrimental effect, with the exception of Mn. This author also reported that, while Ti, V and Cr order antiferromagnetically, Ni and Mn order ferromagnetically. In addition, Mn displays

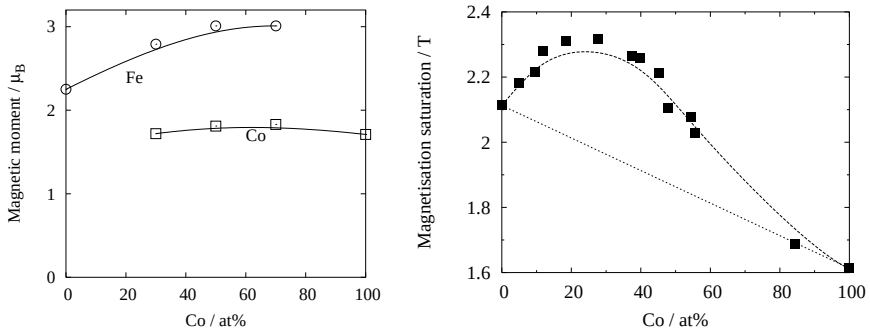

Figure 23: The magnetic moments of Fe and Co on binary alloys of different compositions, after [87]. The saturation magnetisation of $Fe_{1-x}Co_x$ alloys as a function of composition. The straight line is that for an unmilled mixture of pure elements. The formation of a solution is accompanied by an increase in the saturation magnetisation. After [88].

an atomic moment larger than that the average one for FeCo ($\sim 3\ \mu_B$). The case of Mn is further complicated by the fact that its atomic moment depends on the exact stoichiometry of the alloy. It has a simple dilution effect if Fe:Co > 1, only increasing the saturation in alloys where Fe:Co < 1.

This has been further investigated theoretically by Reddy *et al.* [89] using the cluster variation method. Their results also indicate that the impurities Al, V, Mn and Ru preferentially occupy the Fe site, with the substitution of Fe by V being the only one energetically favourable. Chen reports a solubility limit of 7 at% for Mn in FeCo [67] (Köster [49] reporting about 5.5 at%), and the possibility to achieve an average atomic moment of 2.43 μ_B for a 5 at% addition. Mostly because the addition has to be done with excess of Co, the peak reached at 35% Co is not surpassed by that obtained with Mn additions. Few compositions today are found with more than 0.5 wt% (~ 0.48 at%).

Furthermore, similar if not larger saturations have been reported in other ternary alloys by Major and Orrock [81], with 2.44 T (at 4×10^4 A.m^{-1}) for an equiatomic FeCo with 0.23 wt% Nb and 2.45 T for 0.2 wt% Ta.

Saturation is usually regarded as being independent, to a large extent, of the microstructure. Small variations can however be detected; for example, Fingers and Kozlowski [90] report different values of saturation for the same alloy depending on the exact heat-treatment conditions, as illustrated in table 5. Discussion by the above authors appear to imply that such variations are beyond typical error; it must

be noted however that error estimations, when published can reach 0.1 T [19].

Temperature / K	Time / h	Grain size / μm	Saturation induction / T
704	1	1.13	2.37
720	1	1.68	2.40
720	2	2.80	2.43
732	1	2.33	2.40

Table 5: Saturation magnetisation for a FeCo-2V-0.3Nb alloy after different heat-treatments, after [90].

Increasing further the amount of ternary addition leads to significant reduction in saturation, resulting from the both the dilution effect due to the addition of V or Nb, and from the precipitation of non-magnetic particles [24, 28] as illustrated in table 6.

Alloy	Saturation induction / T	Estimated volume fraction of second phase / %
FeCo-2V	2.32	-
FeCo-3.6V	2.29	not measured
FeCo-1Nb	2.34	7
FeCo-2Nb	2.29	11
FeCo-3Nb	2.2	14

Table 6: Saturation magnetisation for different FeCo based alloys after furnace cooling from 760 °C, data from [28].

Similar results have been obtained by Orrock [19] for quaternary systems FeCo-2V-Cu and FeCo-2V-W, where it is shown that the saturation as calculated from the dilution caused by the formation of paramagnetic precipitates (table 11) is in good agreement with measurements, as illustrated in figure 24. This is not the case for FeCo-5Ni [19] or the FeCo-Nb alloys in table 6 where the saturation appears to be larger than expected given the amount of second phase. Orrock suggests that this can occur if the removal of solute causes an increase in average moment in the bulk, that is to say, the loss due to the paramagnetic precipitates is compensated by

a increase of the bulk average atomic moment as the concentration of atoms in solid solution decreases. This is however not a satisfying explanation, since the calculated reference curve mentioned above does not include the solid solution effect in the first place.

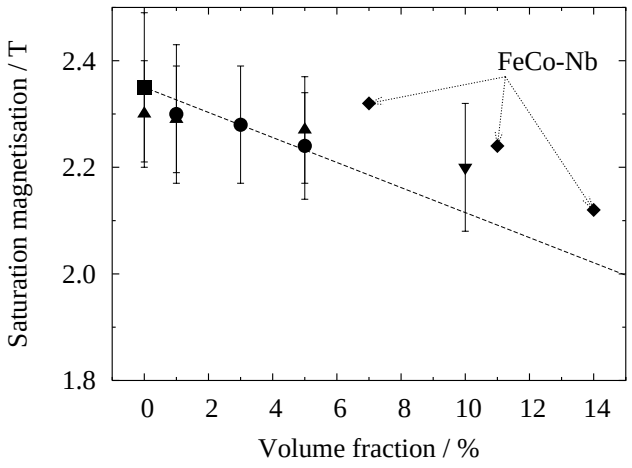

Figure 24: The saturation of a variety of FeCo based alloy as a function of the volume fraction of paramagnetic second phase, after [19, 24]

Error estimates are visible in figure 24 for the data from [19]. Taking into account that some studies have reported saturations up to 2.44 T, it is not evident whether, even for FeCo-Nb, reasons for the differences should be sought elsewhere than in the inaccuracy of the measurements.

4.3 Coercivity

The coercivity is often seen as an important parameter if low losses are to be achieved. It is out of the scope of this review to provide a detailed account of theories relating the coercivity to the microstructure of soft magnetic alloys. The coercivity is, in general, affected by most types of defects. This includes dislocations, grain boundaries, and precipitates.

The coercivity depends on the grain size as follows [31]:

$$H_c \sim 3\sqrt{\frac{kT_cK_1}{aM_s}}\frac{1}{D} \tag{8}$$

where H_c is the coercivity, D the grain size, M_s the magnetisation saturation, K_1 the magnetocrystalline anisotropy, T_c the Curie temperature and a the lattice constant.

The most often quoted relationship between coercivity and non-magnetic particle distribution is due to Kersten [31]:

$$H_c \propto \frac{\delta_w K_1}{M_s \mu_0 \overline{r}} {V_f}^{2/3} \tag{9}$$

where δ_w is the wall thickness, μ_0 the permeability of vacuum, $\overline{r}$ the average radius of the particles and V_f their volume fraction. This does not apply if the wall thickness is greater than the particle size. Néel's approach accounts for the presence of free poles associated with the non-magnetic inclusions, and tend to lead to a linear relationship between the coercivity and the volume fraction of precipitate.

4.3.1 Grain size

In the following section, data from a number of publications have been gathered for comparison. Ideally, the different grain sizes should have been obtained by varying the annealing time at the same temperature, as the concentration of quenched-in vacancies may otherwise vary and affect the result. Clearly, the samples should also be well annealed if comparisons are to mean anything. Figure 25 shows a number of measurements made on a variety of FeCo-X alloys.

In general, the dependency of coercivity on the grain size is in good agreement from one study to another (series (a) to (d) in figure 25), as long as the alloy is well-annealed, single-phase FeCo-X alloy. A satisfying fit is provided by:

$$H_c = 34.2 + 758 \times D^{-1} \tag{10}$$

where D is expressed in μm and H_c in A m^{-1}.

Figure 26 represents the coercivity of a variety of alloys with different grain sizes, in which second-phases were detected. The results obtained by Yu *et al.* [32] for an FeCoV-Nb alloy are somewhat surprising: the coercivity of the sample with smallest grain size appears to fall on the line with the rest of the data, although this particular sample is disordered, and the coercivity of the disordered state is known to be higher than that of the ordered alloy [31]; for the intermediate grain size, an ordered, single-phase sample, the coercivity is significantly lower than for other similar alloys with same grain size, and for the largest grain size, the sample contains

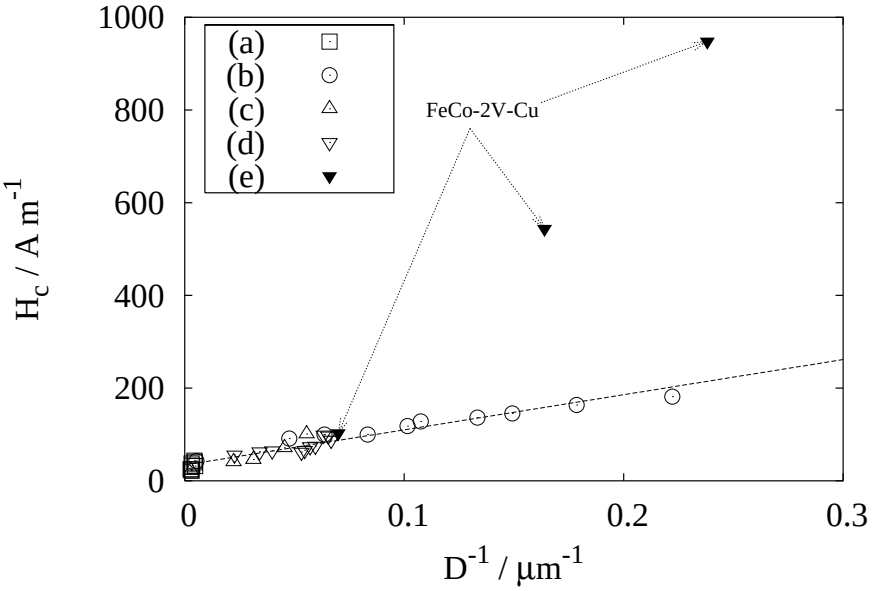

Figure 25: Coercivity of a variety of FeCo based alloys as a function of their grain size. (a) Stanley, 1950, for FeCo-2V [79] (b) Yu *et al.*, 2000, for FeCo-2V [31], (c) Major *et al.*, 1988, for FeCo-0.2Ta [91] (d) Orrock, 1986, for FeCo-2V [19], all are annealed and single-phase. FeCo-V-Cu from [19].

precipitates but nevertheless falls close to the line. Unfortunately, the authors report the amount of precipitates as 3.4 and 2.3 % in the same publication [32] with no indication as to how the volume fraction was estimated.

The FeCo-Nb, FeCo-2V-Cu or FeCo-2V-W alloys, contain varying additions of ternary or quaternary elements, of 1, 2 and 3 wt% (FeCo-Nb) and 1, 3 and 5 wt% (FeCo-2V-Cu and W). As indicated in table 1 and 11, these show increasing amounts of second phase particles.

It is remarkable that the alloys containing 1 wt% of W and Cu fall on the best-fit line determined for single phase FeCo-X alloys. This is consistent with the fact that no significant precipitation is found, and indicates that Cu or W in solid solution do not have a significant impact on coercivity. The case of FeCo-5Ni is particularly surprising as the author [19] reports up to 10% of second phase on grain boundaries.

As discussed in the next section, it is difficult to rationalise the different observations of the effect of precipitation on coercivity.

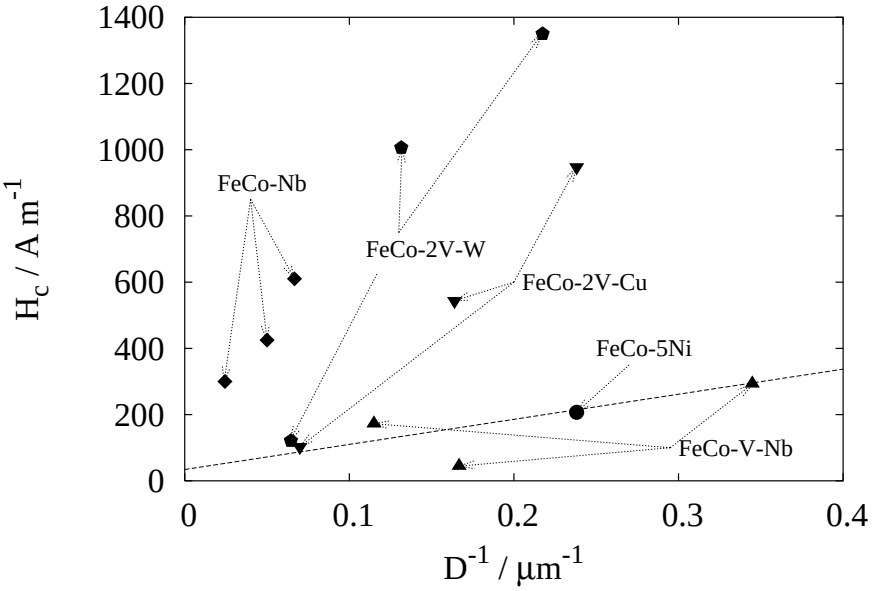

Figure 26: Coercivity of a variety of FeCo based alloys as a function of their grain size. FeCoV-Cu, FeCoV-W and FeCo-Ni from [19], FeCo2V-.3Nb from [32].

4.3.2 Precipitation

It is difficult to isolate the effect of particles on the coercivity, as most tend to influence the grain size. As discussed in the previous section, the precipitates in the large grain sample of FeCoV-Nb (figure 26) do not seem to have a significant impact on the coercivity which falls on the 'universal' line for its given grain size. Unfortunately, the volume fraction reported for this particular case is given, in the same publication [32], as 3.4 and 2.3 %. This is, in any case, of the same order of magnitude as the estimated volume fraction of Cu or γ_2 precipitates discussed later, which cause a very large increase in coercivity.

As illustrated in figure 26, increasing amounts of second phase particles in FeCo-Nb, FeCo-2V-Cu and FeCo-2V-W cause significant increases in coercivity. To isolate the contribution of precipitation, the contribution from the grain size, as predicted from the best-fit line was estimated and subtracted to the actual values reported for these three systems. The results are summarised in table 7. This indicates clearly that consideration on the volume fraction alone cannot explain the different values. For example, the most significant increases are observed in for the FeCo-V-W system which however does not have the largest amount of precipitates. Unfortunately,

Alloy (addition in wt%)	V_f / %	ΔH_c / A m^{-1}	Ref
FeCo-1Nb	7	247	[24]
FeCo-2Nb	11	353	”
FeCo-3Nb	14	525	”
FeCo-1Cu	1	16	[19]
FeCo-3Cu	3	386	”
FeCo-5Cu	5	734	”
FeCo-1W	0	38	”
FeCo-3W	1	872	”
FeCo-5W	5	1151	”

Table 7: The difference (ΔH_c) between observed coercivity and that predicted from the grain size using equation 10 as a function of the volume fraction (V_f) of second phase.

typical particle sizes also appear to be similar between the FeCo-V-Cu and FeCo-V-W systems (~ 0.5 μm, [19]).

Yu *et al.* [31] have reported the changes in coercivity for a W-fibres reinforced FeCo alloy, to which different known volume fractions of Al_2O_3 particles were added (figure 27). Although their results are in good agreement with Kersten's theory, there are a number of reasons to question their validity.

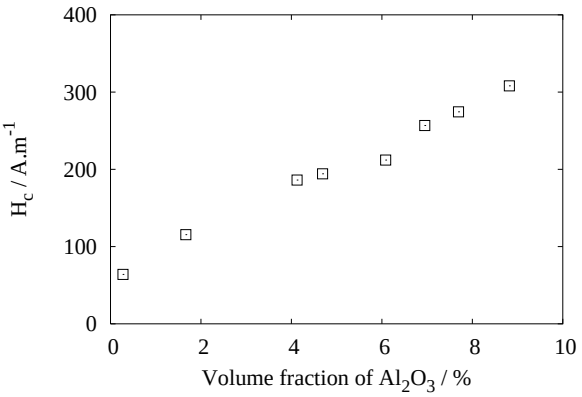

Figure 27: Coercivity of a W-fibres reinforced FeCo, with addition of Al_2O_3 particles in increasing volume fraction, after [31].

A first point is that the theory does not apply to particles smaller than the domain wall. For FeCo alloys, the domain wall thickness has been estimated to ~ 260

nm [31], while Al_2O_3 particles added were ∼37 nm in diameter. In addition, is does not appear that the authors have modified the heat-treatments to ensure identical grain sizes, therefore one cannot exclude that the increase in coercivity mostly relates to a decrease in grain size caused by the Al_2O_3 particles. Furthermore, while these authors represent the coercivity versus $V_f^{2/3}$, a better fit is actually obtained for a linear relationship. It should be noted that Néel's theory would predict a linear dependency, but so would a grain size effect, as it is usually estimated that the average grain size scales with $1/V_f$ when it is controlled by precipitates [92].

Ageing experiments could also provide indirect information on the relationship between coercivity and particle distribution in FeCo based alloys. The evolution of magnetic and electrical properties during ageing is a recent concern and few studies have been undertaken [31, 35, 62, 71]. These are discussed in greater detail later. Unfortunately, The authors have not correlated the changes in magnetic properties with microstructural evolution, so that once again, a quantitative assessment of the respective roles of grain size and precipitation is not possible.

A careful, quantitative investigation of the relationship between coercivity and microstructure should therefore include measurements of grain size distribution and particle distribution. It appears quite clearly from the above that the correlation between microstructure and coercivity remain unclear, further investigations should include not only grain size measurement but also second phases distribution.

4.3.3 Deformation

As mentioned in the introduction, coercivity is, in general, affected by any type of defects. The impact of a deformed microstructure is clear when considering partially recrystallised microstructures. FeCo base alloys are typically cold-rolled after quenching, then annealed at temperatures around 700-800 °C. A number of authors have pointed out the possibility of obtaining a high strength material if the annealing treatment is carried out at lower temperatures.

Thornburg [59] varied the annealing temperature for a commercial FeCo-2V alloy after cold-rolling to 90% thickness reduction, and showed that coercivity dropped sharply with increasing temperature until full recrystallisation. Above this temperature, only the differences in grain size caused relatively small changes in comparison. Similar results were obtained by Hailer [93] for FeCo-2V-0.3Nb, as illustrated in fig-

ure 28.

As for the strength 5.1.4, the present authors recently showed, using published data on grain growth [57], that these variations could be entirely explained by changes in the grain size. Figure 28 shows a comparison of measured and calculated coercivity, the details of the calculation have been published elsewhere [61].

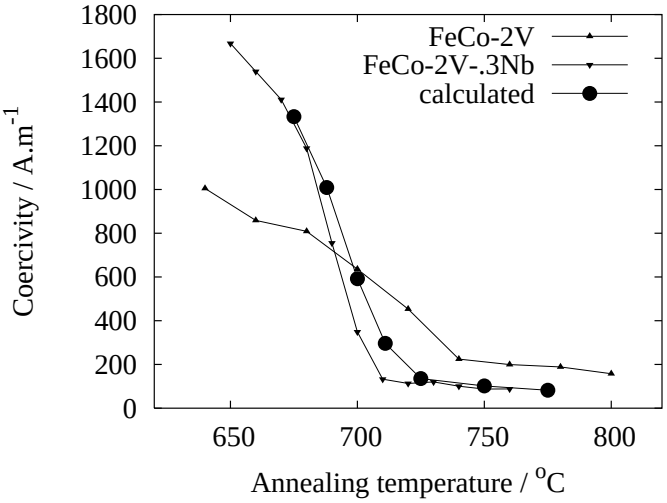

Figure 28: Coercivity of FeCo-2V [59] and FeCo-2V-0.3Nb [93] after annealing at different temperature, for 1 h in the case of FeCo-2V-0.3Nb, 2 h for the FeCo-2V alloy. Exact measurement conditions are not indicated in [59]; for FeCo-2V-0.3Nb [93], coercivity was measured with maximum applied field of 1.59 T, at 60 Hz. This is compared with calculations for FeCo-2V using equation 10 and the grain sizes reported by Davies and Stoloff [57].

4.4 Permeability

As mentioned earlier, the use of equiatomic FeCo alloys as opposed to lower Co content is mainly driven by their very high permeability. There is surprisingly little studies reporting directly either the initial or maximum permeabilities of FeCo based alloys.

Although there is evidence for a decrease in permeability in FeCo-2V during long-term exposure to intermediate temperatures (450-550 °C) [71], one can only speculate, for lack of direct evidence, that this is a consequence of γ_2 precipitation as observed by Ashby *et al.* and discussed in section 2.2.2.

The impact of Cu and W additions in FeCo-2V alloys on their coercivity has been discussed above. Orrock also reports saturation for different applied fields, showing a significant decrease in permeability, even for additions which had no impact on coercivity, as shown in table 8.

	FeCo-2V	FeCo-V-Cu			FeCo-V-W		
		1	3	5	1	3	5
$M_{4000A.m^{-1}}$	2.23	1.99	1.90	1.65	1.79	1.73	1.69
$M_{40000A.m^{-1}}$	2.34	2.28	2.23	2.18	2.20	2.19	2.19

Table 8: The magnetisation at 4000 and 40000 A.m^{-1}, showing that, while saturation is little affected by the addition of Cu or W to FeCo-2V, the magnetisation at intermediate applied fields is significantly reduced. After [19].

Works on FeCo-V-Ni [42, 43] indicate a detrimental effect on the permeability: the maximum permeability of this alloy, after optimum heat-treatment, is found to be about 2.5 times lower than that of FeCo-2V. A similar observation was made on FeCo-Nb alloys [24], with FeCo-1Nb wt% showing a maximum permeability about 3 times lower than FeCo-2V. Unfortunately, there is no investigation of the differences in microstructure in these studies.

4.5 Resistivity

The resistivity of FeCo based alloys is as important as the magnetic properties in the obtention of low losses components. Ordered binary FeCo has particularly low resistivity as shown in table 9. By coincidence, the addition of vanadium, as proposed by White and Whahl [3] to improve the ductility, would later be shown to be the most efficient way to improve the resistivity of these alloys, as illustrated in figure 29.

As discussed later, Nb and Ta have recently been shown to provide interesting replacement for vanadium, as they impart ductility even for much smaller additions. However, as illustrated in table 29, these additions do not have the same impact as vanadium on the resistivity; in fact, the resistivity of FeCo-Nb is hardly different from that of the binary system.

The temperature dependency of the resistivity of FeCo-2V (Hiperco H50) and

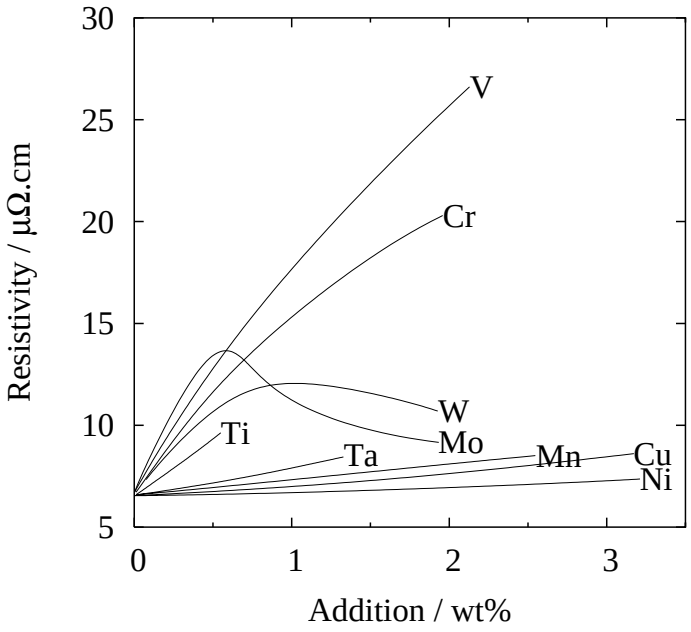

Figure 29: The influence of various addition on the resistivity of FeCo alloys. After [67].

FeCo-2V-Nb (Hiperco H50HS) has been investigated by Geist *et al.* [35]. and that of FeCo-Ta (48.75 Co, 0.45 Ta, 0.27 V wt%) by Simon *et al.* [94]. This is illustrated in figure 30.

According to [35], the detailed content of the alloys investigated are, 48.75 Co, 1.9 V, 0.05 Nb (wt%) for H50, and 48.75 Co, 1.9 V, 0.3 Nb for H50HS. While both alloys appear to have the same amount of vanadium, there is a significant different in resistivity. As discussed in section 6, it can be suggested that this is caused by promotion of γ_2 formation in the high Nb alloy. If the V-rich γ_2 compound precipitates early, less vanadium remains in solid-solution to increase the resistivity.

Alloy	Resistivity / $\mu\Omega$.cm
FeCo	1.95
FeCo2V	46.4
FeCo1Nb	3.13
FeCo2Nb	3.06

Table 9: The resistivity of FeCo and FeCo-V and FeCo-V-Nb alloys, after [24].

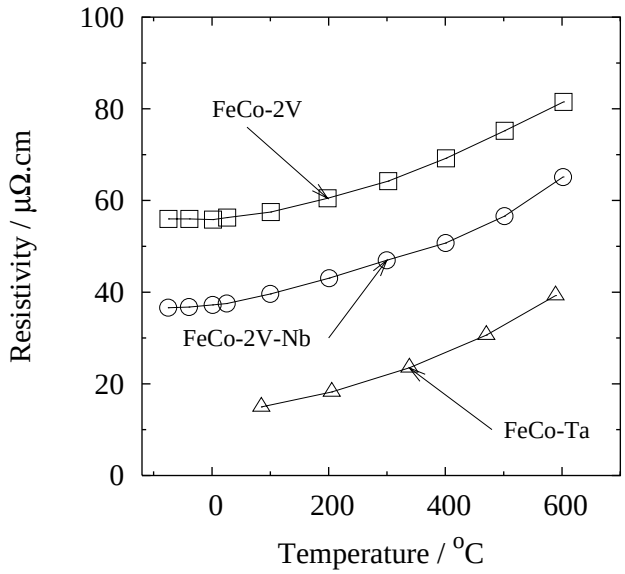

Figure 30: The resistivity of FeCo-V, FeCo-V-Nb and FeCo-Ta as a function of temperature, after [35] and [94].

5 Mechanical properties of Fe-Co based alloys

The mechanical properties of FeCo base alloys have been the object of a number of studies, particularly in the context of ordering.

5.1 Yield Stress

As for most metallic alloys, the yield stress of FeCo based alloys can vary considerably depending on thermomechanical treatment and composition, and it is therefore difficult to discuss it out of context. In the following section, the influence of a number of parameters are reviewed.

5.1.1 The influence of order/disorder

The present review does not explore the dislocation theory in depth and the author recommends, for example, the review of Marcinkowski [95] for further details.

To investigate the influence of the degree of long-range order (S) on the yield stress, Stoloff and Davies [75] quenched tensile specimens from temperatures in the range 500 to 875 °C, having established independently the corresponding degree of order. As illustrated in figure 31, the yield stress exhibits a peak for quench temperatures slightly below the critical temperature (corresponding to $S \sim 0.4$ according to Stoloff and Davies). Identical results have been obtained by Marcinkowski and Chessin [96] and Moine *et al.* [97] (shown in figure 31).

Note that the samples quenched from $T > T_c$, in theory disordered, exhibit a higher strength than the ordered ones. Although the size of the samples used by Stoloff and Davies (tensile samples of 3.2 mm diameter) is significantly above the critical dimension identified by Clegg and Buckley (section 3.2.2) for complete retention of disorder through quenching, similar results have been obtained by a number of authors, in particular, Ren *et al.* [58] have performed tensile tests of coupons taken from 0.35 mm sheets of FeCo-2V alloy and obtained the values reported in table 10.

Marcinkoswski [95] attributed the high strength of the disordered alloy to a high degree of short range order (SRO). Comparing FeCo and Ni_3Mn, Marcinkowski suggested that the high ratio T_c/T_m (T_c ordering temperature, T_m melting temperature) renders difficult the retention of disorder through quenching of FeCo based mate-

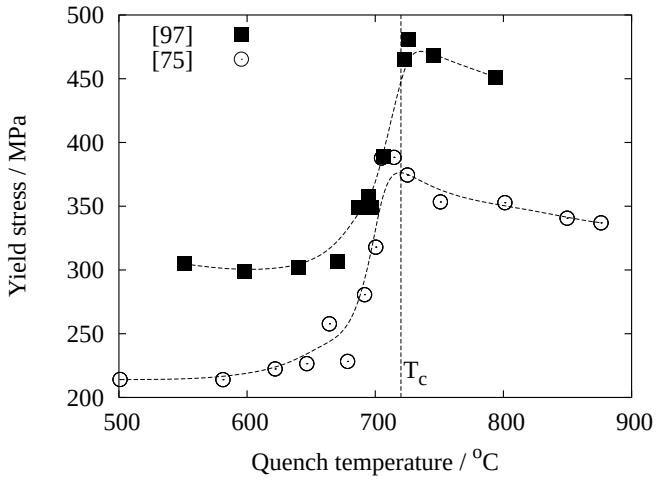

Figure 31: The 0.1% yield stress for FeCo-2V samples quenched from different temperatures so as to produce different degree of long range order, after [75] and [97].

Cooling rate °C/h	30	60	90	Air quenched	I.B. quenched
Yield Stress / MPa	389	359	385	503	526

Table 10: The yield stress of FeCo-2V quenched from 820 °C at different rates. The three slow cooling treatments lead to ordered specimen with possibly varying grain size, both quenching methods lead to disordered specimen (I.B.: iced brine). After [58]

rials, as materials with a lower T_c/T_m such as Ni_3Mn show a lower strength in the disordered state than in the ordered one.

Stoloff and Davies [75] explained the influence of order-disorder on σ_y by suggesting that a peak in strength would occur as the transition between deformation by single dislocations to superlattice dislocations takes place. While single dislocations face increasing resistance as S increases, superlattice dislocations are not sensible to the degree of order.

A number of studies have reported a change in deformation mode from wavy to planar as the system orders [75,96,98]. Results concerning the preferred slip systems tend to agree for the disordered system, where slip is reported to occur on {110}, {112} and {321} type planes, but agreement is poor for the ordered system: results from Jordan and Stoloff [98] opposed the common assumption [75, 99] that slip is restricted to {110} type planes for the ordered system, as the authors identified

predominant slip on either {321} or {211} planes depending on the temperature. Yamaguchi *et al.* [100] , however, studied deformation of ordered single crystal FeCo at 4.2, 295 and 600 K, and reported a strong preference for slip on {110} at all temperatures.

The existence of the transition from planar to wavy glide, near the peak strength, was taken by Stoloff and Davies [75] as supporting their proposed mechanism: slip is dominated, at none or low degree of LRO, by single dislocations which face increasing resistance as the degree of order is increased; as the degree of LRO increases, slip is increasingly dominated by superlattice dislocations and the strength decreases (figure 32).

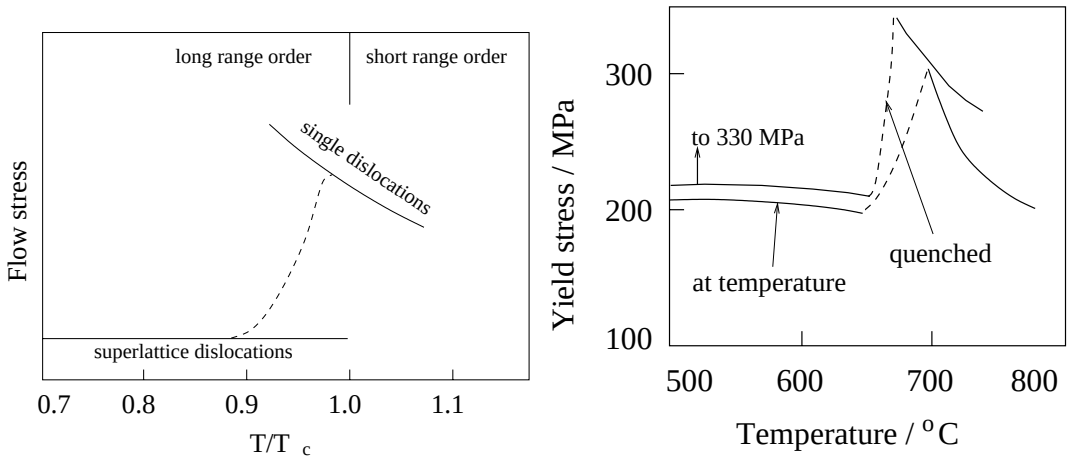

Figure 32: Illustration of the mechanism proposed by Stoloff and Davies to explain the influence of order/disorder (and of temperature through order/disorder) on the yield strength of FeCo based alloys, after [75]. Predictions by Moine *et al.*, for yield strength measured at indicated temperature and after quenching from the indicated temperature, after [97]. Note that the curve for quench temperature has been shifted to lower values for easier comparison.

Moine *et al.* [97] noted that superlattice dislocations are found even in alloys quenched from above T_c. These authors then proposed a quantitative analysis of the problem based on the stress required to activate Franck-Read sources for single and superlattice dislocations. They obtained, for high values of S where the dislocations remain paired:

$$\sigma_y = \alpha \frac{\mu b}{\pi l_0} \left(\ln \frac{l_0}{b} + \ln \frac{l_0}{r_c} + \frac{\alpha_0}{\alpha} \right) \tag{11}$$

and, for low values of S where the Franck-Read source functions with single dislo-

cations:

$$\sigma_y = \alpha \frac{\mu b}{\pi l_0} \left(\ln \frac{l_0}{b} + \frac{\alpha_0}{\alpha} \frac{l_0}{r_c} \right) \tag{12}$$

where σ_y is the yield stress, α and α_0 are geometric factors, b is the burgers vector, μ the shear modulus, l_0 the length of dislocation between pinning points and r_c the distance between paired dislocations (depending on the SRO and LRO).

The link between the observation of superlattice dislocations above T_c and the proposed mechanisms is not clear; in fact, rather than opposing the views of Stoloff and Davies, this analysis seems to provide support for it, as noticed by Marcinkowski [95]. Furthermore, although the predicted strength offers good agreement with measurements, the published work leaves unclear a number of important points, in particular that of the variation of short-range order with temperature above T_c, which is, according to the model, essential in understanding the high strength of the disordered state and its temperature dependency: the model does not incorporate explicit temperature dependence but through the LRO and SRO parameters. Finally, the difference between tests carried at high temperature or after quenching is only introduced in the model through a change in l_0 whose physical meaning is not clear.

Recent theories have focused on the role of vacancies, and have mostly been discussed in the context of the temperature dependence of the yield strength.

5.1.2 The influence of temperature

The interpretation of results on the influence of test temperature on the flow stress are complicated by the fact that the degree order can only be kept constant over a small interval of temperature. Jordan and Stoloff [98] , for example, have performed a study of the temperature dependence of the yield stress for ordered and disordered FeCo-2V alloys; to retain the disorder or a constant degree of LRO, the temperature was kept within 77 and 300 K, and 77 and 773 K respectively. Most other studies cover a range of temperature where change in the degree of LRO is expected.

The temperature dependence of the yield strength resembles that for the order-disorder. As the temperature increases, the strength goes through a peak located near the critical temperature for ordering. However, there is significant variations in the literature over the amplitude of the peak, as illustrated in figure 33.

Results from Moine *et al.* [97] for strain rates of 3.375 s^{-1} and 0.0375 s^{-1} suggest

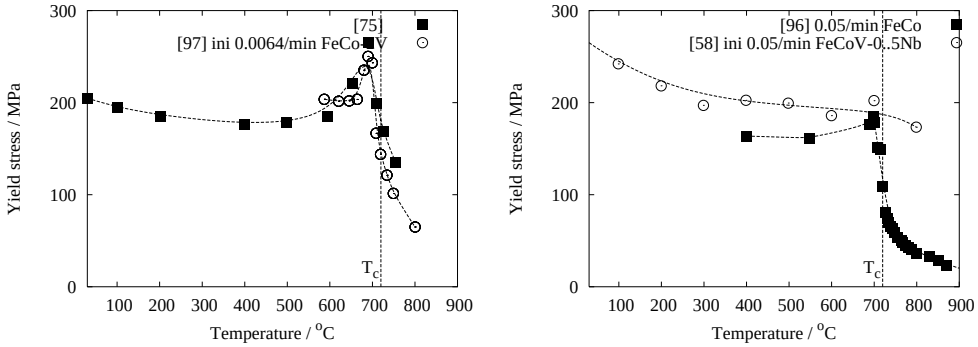

Figure 33: Variation of yield strength with temperature (a) for FeCo-2V [75, 97] showing significant increase of strength as the temperature increases to the critical temperature for ordering, (b) for FeCo [96] and FeCo-2V-0.03Nb [58] showing little increase of strength before the T_c.

that the position and amplitude of the peak is independent of strain rate. While the difference between the behaviour of FeCo-2V (figure 33a) and FeCo (figure 33b, [96]) might be attributed to the different compositions, the entirely different behaviour reported by Ren *et al.* [58] is difficult to explain. The author proposes that the particularly small grain size of their samples could explain the little pronounced peak, without further clarification. However, it should be noted that while all the first three studies discussed above [75, 96, 97] emphasise the need to allow time to equilibrate at high temperature in their experimental procedures, this is not mentioned in [58] and it is therefore possible that Ren *et al.* have overlooked this issue. In ordered FeAl (also a B2 structure), the yield stress anomaly can be hidden by quenched-in vacancies if the samples are not equilibrated at the test temperature [101]; in fact, the general shape of the curve σ_y vs temperature resembles, in this case, the one obtained by Ren *et al.* [58].

Stoloff and Davies [75] or later Moine *et al.* [97] have supposed that the same mechanism (change from superlattice dislocations to single dislocations as discussed in the previous section) should explain both curves, that is to say the effect of quenching temperature (figure 31) and the effect of test temperature (figure 33).

The strength of B2 ordered compound has been mostly studied using FeAl, and a variety of models have been proposed to explain the yield stress anomaly in these alloys (for example [101–111]). This is out of the scope of this review but a brief mention will be made of the two most recent models: Morris [102] proposed a mechanism whereby the increase in strength occurs as a result of local locking of

super-dislocation by climb, as transfer of vacancies occurs from one to the other, and the decrease occurs when the slip system changes, in the case of FeAl to <100> dislocations. Perhaps the most serious criticism against this mechanism, as raised by George and Baker [106], and which would also hold for FeCo alloys, is that, while it would predict a decrease in strength with increasing strain rates in the temperature region where the locking occurs, experimental evidences (FeAl: [106], FeCo: [97]) show no such influence. Other difficulties concern the composition dependence of the peak temperature and the glide transition temperature [101].

In George and Baker's model [106, 107] , the increase in strength at intermediate temperatures is caused by increasing vacancy generation, while the decrease, at higher temperature, occurs when their mobility is sufficient to allow dislocation climb. Although this model has given satisfactory agreement with observations, it has recently been criticised by Kupka [111], whose results indicate that the yield strength peak cannot, or not entirely, be explained by vacancy hardening, this author further points to a number of discrepancy with other results in the literature. It should also be noted that this model ignores the copious amount of experimental evidence for a change from <111> to <100> type dislocation, which occurs at temperatures close to that of the peak strength [102]. Figure 34 explains schematically the differences between the mechanisms.

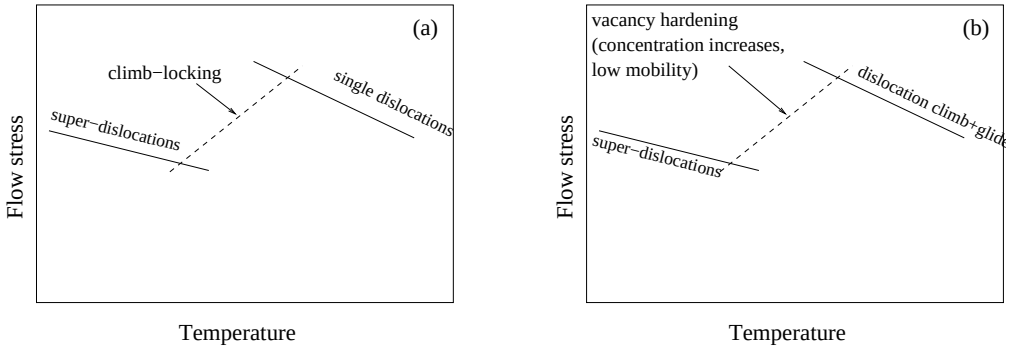

Figure 34: Schematic illustration of the mechanism proposed by Morris [102] (a) and George and Baker [107] to explain the peak strength of FeAl at intermediate temperatures.

In the case of FeCo alloys, both mechanisms suffer a number of shortcomings: while that of Morris takes into account the observed change of glide system, it is clearly inapplicable to room temperature tests of quenched samples, as it relies on thermally activated vacancy movement from one dislocation to the other in a

super-dislocation. The peak is nevertheless observed in room temperature tests of quenched alloys.

The model of George and Baker would, on the other hand, explain the increase for both kind of tests, since the concentration of quenched-in vacancies increases as the quench temperature increases, however the climb-glide mechanism proposed to explain the decrease is once again inappropriate for room-temperature tests of quenched samples; furthermore, as for FeAl, it ignores the change of glide system. In addition, it predicts a shift of the peak to higher temperatures as the strain rate is increased; while this has been reported in FeAl [108, 110], results by Moine *et al.* [97] have obtained similar peak for significantly different strain rates, both for the room temperature tests of quenched samples and for the high-temperature tests.

There would be a number of ways in which one could 'fit' an explanation to the observed phenomena borrowing from one mechanism or the other; for example, accept the vacancy hardening proposed by George and Baker for the increase of strength, but rely on the glide system change to explain the drop.

However this would remain entirely speculative given the lack both of quantitative predictions and of experimental data in the case of FeCo alloys. It is likely that a proper quantitative model will include both aspects (role of vacancies and change of slip mode) of the problem; presumably, part of the complexity of the problem and lack of agreement comes from the fact that both factors could play roles of similar importance.

Much work therefore remains to be done to understand clearly the origin of the yield anomaly and establish whether mechanisms established for FeAl may apply.

5.1.3 The influence of grain size, composition and precipitates

Grain size, composition changes and precipitation are closely related, as, most often, the presence of second-phase strongly affects the recrystallisation kinetics so that vastly different grain sizes can be obtained after identical heat-treatments. It has also been proposed that some additions have an important impact through solute drag effect, such as Mn [112].

A number of studies have demonstrated that, for most of the FeCo based alloys currently in use, the strength is mainly controlled by the grain size (that is, for annealed, ordered samples at a given temperature), while little influenced (directly)

by solid solution or precipitates.

Most of the results have been interpreted using the Hall-Petch relationship:

$$\sigma_y = \sigma_0 + kd^{-1/2} \tag{13}$$

where σ_0 and k are constants.

In a recent study, Shang *et al.* [33] have investigated the grain size dependency of three different FeCo based alloys: FeCo-2V, FeCo-2V-Nb (Hiperco H50HS) and Fe-27Co. Their results (figure 35) indicate that the presence of second-phase precipitates in H50HS does not contribute directly to the strength as the hardness of all three alloys falls on the same Hall-Petch line. These precipitates do however explain the higher strengths of these alloys in as much as they inhibit grain-growth during the annealing treatment.

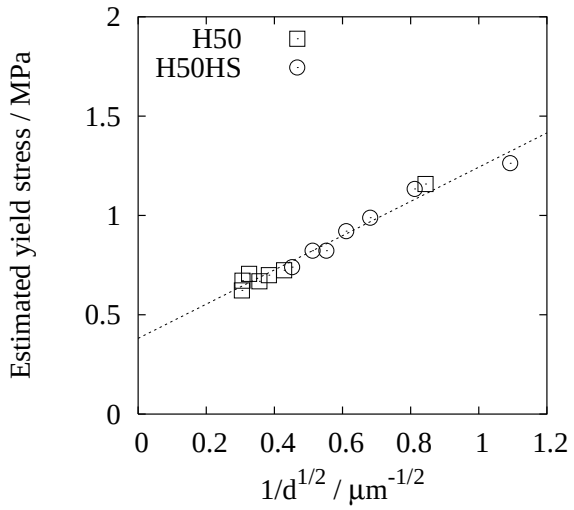

Figure 35: The grain size dependence of FeCo-2V (H50) and FeCo-2V-Nb (H50HS) showing a unique Hall-Petch line regardless of the fact that the latter alloy contains second-phase precipitates, after [33].

Unfortunately, the authors [33] obtained different grain-sizes (not reported) by annealing treatments of different duration at temperatures between 700 and 800 °C. It is also not specified whether the samples were quenched or slow-cooled. In the former case, little can be deduced from the results as one would expect significant impact of quenched-in vacancies, if not order/disorder. These results are not used in the comparison to follow, as they were obtained by hardness measurements rather than tensile of compression tests.

To examine the problem further, the present author gathered data from a variety of publications, for FeCo based alloys with various additions and different heat-treatments, provided they were tested in fully recrystallised, ordered state. Figure 36 shows the strength of a number of alloys versus their grain-size.

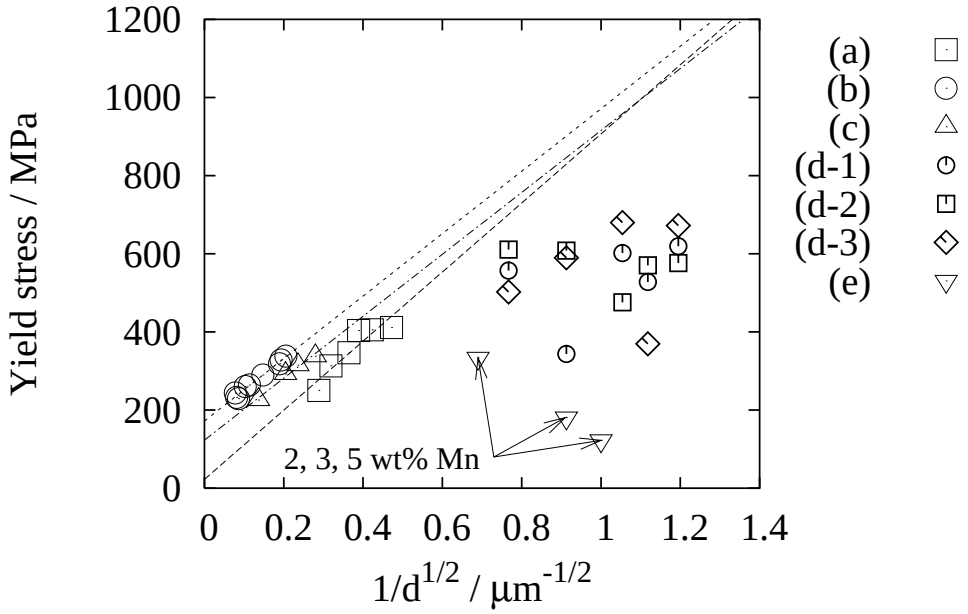

Figure 36: The strength of a variety of FeCo based alloys in well annealed, ordered condition. (a) FeCo-2V-.05Nb held for different times at 820 °C [58]; (b) FeCo, 2 h at 850 °C, 10 h at 500 °C then furnace cool to room temperature, grain size variation from prior condition [91]; (c) FeCo-2V held for different times at 850 °C, 5 h at 500 °C then slow cooled to room temperature [98]; (d) different compositions of FeCo-V-Ni, held 2 h at temperature between 650 and 750 °C to produce different grain sizes, then cooled to room temperature at 90 °C/h: (d-1) FeCo-1.5V-4.5Ni, (d-2) FeCo-1.5V-5.3Ni, (d-3) FeCo-0.7V-7.4Ni, [112]; (e) FeCo-V-Mn alloys held 2 h at 700 °C then cooled at 90 °C/h to room temperature [112].

In the case of Ni additions to the FeCo-2V system (series (d)) [112, 113], the authors report identical grain sizes and amount of γ_2 for different addition of Ni between 3.5 and 7.4 wt%, both parameters being only dependent on the annealing temperature. As the annealing temperature is decreased, so is the grain size and the amount of γ_2. As mentioned earlier (section 2.2.3), adding Ni to FeCo-2V stabilises γ_2 which is normally not present after annealing around 700 °C, this results in smaller grain sizes. However, above 3.5 wt%, there is no increase in the amount of γ_2 precipitated. Considerable scatter in the measurements of the yield stress for

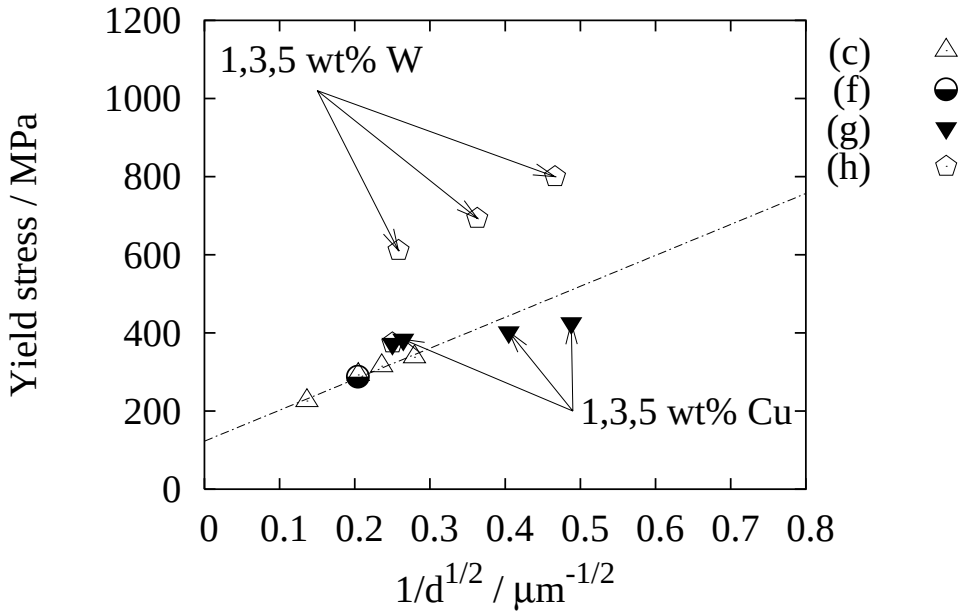

Figure 37: The strength of a variety of FeCo based alloys in well annealed, ordered condition. (c) as for figure 36; (f) FeCo-2V held 1 h at 825 °C then 24 h at 550 °C, 48 h at 500 °C the slow cooled to room temperature [82];(g) FeCo-2V-Cu held 2 h at 850 °C then slowly cooled at 120 °C/h [19]; FeCo-2V-W, similar heat-treatment [19].

these alloys make it difficult to draw any conclusions as to the influence of the grain size and/or precipitation, but it is noticeable that all fall below the extrapolated values from any of the three FeCo-2V-.05Nb (a), FeCo-2V (b) and FeCo (c).

The case of Mn additions (series (e) in figure 36) is interesting, as, according to Pitt [112] increasing amounts of Mn (2, 3 and 5 wt%) lead to reduced amounts of second-phase after a standard heat-treatment of 2 h at 700 °C and slow cool. In correlation, the grain size is greatest for the alloy with 5 wt% Mn and smallest for the 2 wt% addition, nevertheless, the yield stress is greater for the 5 wt% addition, which may indicate solid solution strengthening. However, it must be noted that these samples were not, according to Pitt, fully recrystallised; the author further reports slower recrystallisation kinetics with increased Mn content. It is therefore equally possible that work-hardening explains the trend observed for FeCoV-Mn samples.

The impact of copper and tungsten additions have been investigated by Orrock [19]. In this case again, variations of grain size are caused by increasing amounts

of second phase. The results of microstructural investigation (table 11) indicate increasing presence of second-phases in both cases, which cause a decrease in grain-size.

Figure 37 illustrates the results obtained by Orrock for FeCo-2V-Cu (series (g)) and FeCo-2V-W (series (h)). All samples are fully recrystallised, having been annealed 2 h at 850 °C, then cooled at 120 °C/ h to room temperature.

	1wt%	3 wt%	5 wt%
FeCo-2V-Cu	$d \sim 14.3$ μm, about 1% Cu precipitates	$d \sim 6.1$ μm, about 3% Cu precipitates	$d \sim 4.2$ μm, about 5% Cu precipitates
FeCo-2V-W	$d \sim 15.0$ μm, no second-phase	$d \sim 7.6$ μm, about 1% grain boundary γ_2	$d \sim 4.6$ μm, about 5% grain boundary and intragranular γ_2

Table 11: Results of Orrock's microstructural investigation on FeCo-2V-Cu and FeCo-2V-W, after [19].

While the copper leads to little improvement in strength, the effect of tungsten is particularly interesting: the increase in strength obtained with only 1 wt% indicates that solid solution is the main cause of strengthening, furthermore, the grain size dependence appears similar to that of FeCo-2V (series (c)), which indicates that the increasing amount of second-phase has negligible impact on the yield stress.

Recently Duckham *et al.* [65] investigated the mechanical properties of FeCo-2V-0.5Nb with sub-micron grain sizes. As illustrated in figure 38 their results, for grain sizes between 100 nm and 1.6 μm fall reasonably close to the extrapolated values for FeCo-2V or FeCo-2V-Nb, although obtained on grain sizes at least an order of magnitude greater.

Jordan and Stoloff [98] have obtained a variety of grain sizes in an FeCo-2V alloy by varying the annealing time at 850 °C, after cold-rolling. The samples were either quenched in ice brine (disordered) or quenched and re-heated for 5 h at 550 °C (ordered). They report the Hall-Petch parameters at a variety of temperatures (figure 39).

In both the studies whose results are illustrated in figure 39, the numerical values for the grain size are identical for the ordered and disordered samples. Given the unlikeliness of obtaining identical results even on similar samples, one has to suppose

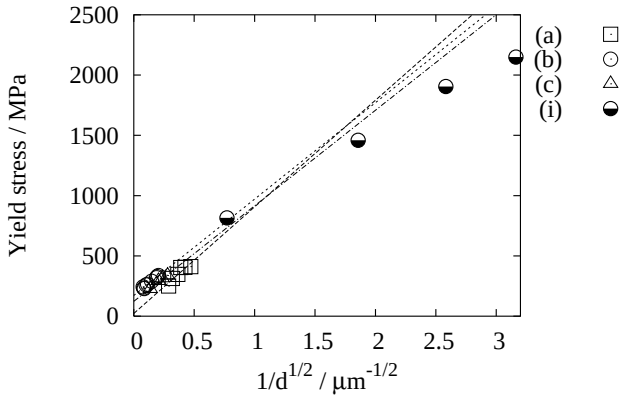

Figure 38: The strength of FeCo-2V-0.5Nb with sub-micron grain size. Series (a) to (c) as in figure 36 and 37; (i) data from Duckham *et al.* [65].

that the grain size was measured after the annealing treatment, and assumed to be identical in samples receiving a further ordering heat-treatment at 500-550 °C. It should be noted however that Pitt and Rawlings [113] have reported some grain growth even at these temperatures, with an increase from 30 to 37 μm over 10-30 hours at 550 °C (and further to 80 μm after 11 days). Yu *et al.* have reported grain growth during conventional slow cooling from 820 °C (90 °C/h) [66].

Other reported values of Hall-Petch parameters are shown in table 12. The difference in σ_0 and k can be visualised in figure 36 (series (a), (b) and (c)), which shows clearly that the significant variations, particularly in σ_0 might be only the result of scatter in the data.

Influence of order/disorder on σ_0 and k All studies show that, while σ_0 is larger for disordered samples, these also have a lower k. While σ_0 relates to the lattice friction, k relates to the difficulty of operating a dislocation source across a grain-boundary [114].

It has been proposed [95] that the larger values of k in ordered alloys relates to the higher stresses required to operate a dislocation source in the ordered material, and the reduced number of slip planes available for super-dislocations. This observation contradicts the calculations of Moine *et al.* [97] discussed earlier, which lead to the conclusion that dislocation sources are more difficult to operate in disordered alloy.

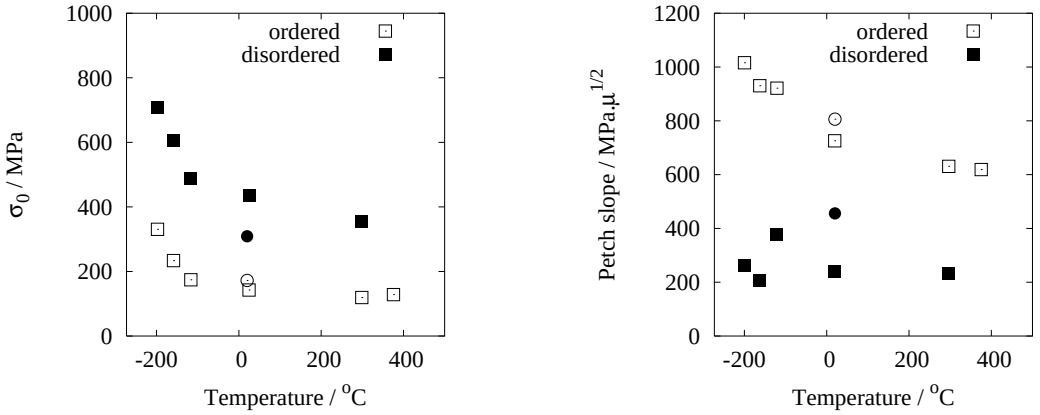

Figure 39: The Hall-Petch parameters σ_0 and k as measured by Jordan and Stoloff for FeCo-2V at different temperatures [98]. Superimposed (circles) are the results of Zhao and Baker for FeCo *et al.* [91] at room temperature.

The influence of precipitation From the above, and particularly figures 36 and 37, it can be seen that precipitation appears to have no direct impact on strength. Quite surprisingly, the alloys with significant precipitation tend to have the same or lower strength than those void of second-phase particles (FeCo-2V-Ni, FeCo-2V-Cu).

Yu *et al.* [31] have recently reported the hardness of FeCo samples with dispersions of Al_2O_3 particles and observed an increase in strength scaling with $V_f^{1/3}$, however, the authors do not appear to have varied heat-treatment to ensure identical grain sizes, so that the observed increase in yield stress is likely to be have been caused by grain refinement.

5.1.4 Influence of heat-treatment

The problem of recrystallisation and grain-growth is discussed in a later section. The impact of heat-treatment on strength has been studied by Thornburg [79] for FeCo-2V, and more recently Hailer, for FeCo-2V-0.3Nb [93]. Specimen of the former had been cold-rolled to about 90% reduction in thickness; although not specified for the latter, the origin and nature of the samples (Hiperco H50Hs, Carpenter alloys) suggest that they had been cold-rolled to similar extent.

As illustrated in figure 40, there is a sharp decrease at what has been interpreted by the two authors as the temperature at which recrystallisation is complete in the given time.

Composition	Peierls stress / MPa	k / MPa.μm^{-1}	Method	Reference
FeCo				
ordered	172	806	compression	X35: [91]
disordered	309	456	tests	
FeCo-2V				
ordered	143	714	tensile	X36: [98]
disordered	435	242	tests	
FeCo-2V				
ordered	26	848	tensile tests	X27: [58]
Fe-27Co, H50, H50HS				
ordered (?)	404	837	Knoop hardness	X2: [33]

Table 12: Different values of σ_0 and k for ordered and disordered samples of FeCo based alloys.

However, the present author recently showed [61] that this sharp changes could be attributed to the significantly different rates of grain growth below and above the critical temperature for ordering.

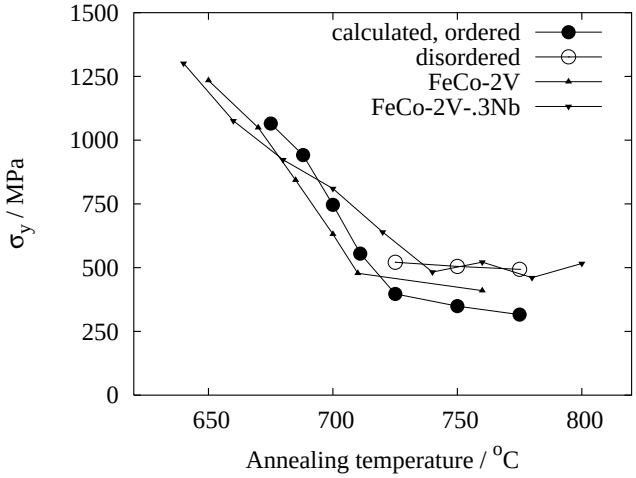

Figure 40: The strength of FeCo-V and FeCo-V-Nb alloys, as measured by Thornburg [59] and Hailer [93] respectively. Calculation for FeCo-2V using the grain sizes reported by Davies and Stoloff [57], assuming in a first instance, that all samples are ordered (filled circles), and in a second study, that samples cooled from above T_c are disordered (empty circles).

Figure 40 and compare the strength and coercivity as measured by Thornburg for

FeCo-2V [59] and by Hailer [93] for FeCo-2V-0.3Nb, and calculated by the present authors using the grain size data from Davies and Stoloff [57]. Details of the calculation have been published elsewhere [61].

5.2 Ductility

There has been a tendency to associate brittleness with order and ductility as evidence of disorder. There is increasing evidence, however, that this viewpoint is not correct.

5.2.1 Ductility of binary alloy

The binary equiatomic FeCo is notoriously brittle, particularly in the ordered state. However, few studies have dealt with this alloy, with the main body of the literature concerning the ternary FeCo-2V. Some of the results are summarised in table 13.

Alloy	Condition	Elongation	Fracture	Reference
Fe-50Co	ordered (2 h at 800 °C + 10 h at 550 °C)	4%	Mostly intergranular with few transgranular facets	[75]
”	disordered (2 h at 800 °C + IBQ)	0%	”	”
Fe-49.3Co	ordered (heat-treatment details unknown)	1.6%	Entirely transgranular	[96, 115]
”	disordered (as above)	0%	Entirely intergranular	”

Table 13: Some results on elongation and fracture mode for binary FeCo alloys.

Yamaguchi *et al.* [100] (Fe-54Co) reported plastic deformation of single crystal FeCo at temperatures as low as 4.2 K, while the polycrystalline material fractured solely by intergranular fracture in similar conditions. Glezer and Maleyeva also reported entirely intergranular fracture for FeCo [116]. More recently, George *et al.* also reported intergranular fracture in both ordered and disordered samples of binary FeCo [82].

The cause of the brittleness of the ordered alloy has been the subject of much discussion. The link with the ordering reaction has been long established: the brittleness falls in the same range as the ordering reaction [17, 79], in addition,

heat-treatments or additions which are believed to delay ordering tend to improve ductility, as discussed later.

It is clear, that FeCo alloys are particularly sensible to intergranular fracture. The role of vanadium additions in enhancing the ductility sheds further light on the problem, and is discussed before proposing a summary.

5.2.2 Influence of vanadium additions

The FeCo alloy as introduced by Elmen (1929, [2]) remained without extensive industrial application until the introduction of the FeCo-2V by White and Wahl [3], mainly because of the difficulties caused by its brittleness in working or machining. White and Wahl (1932, [3]) realised that additions of vanadium, with an appropriate heat-treatment, led to a material that could be cold-rolled. While a 1.5 wt% was not sufficient, a 2% addition allows a material quenched from $\sim$ 900 °C in iced brine to be cold-rolled. With increasing vanadium, air quench becomes sufficient and the temperature of the heat-treatment needs not be as accurate.

Stoloff and Davies [75] reported the ductility of Fe-48Co-2V samples quenched from a range of temperatures; as illustrated in figure 41. From comparison with other results [68], it appears that these times are largely sufficient to reach the equilibrium degree of order.

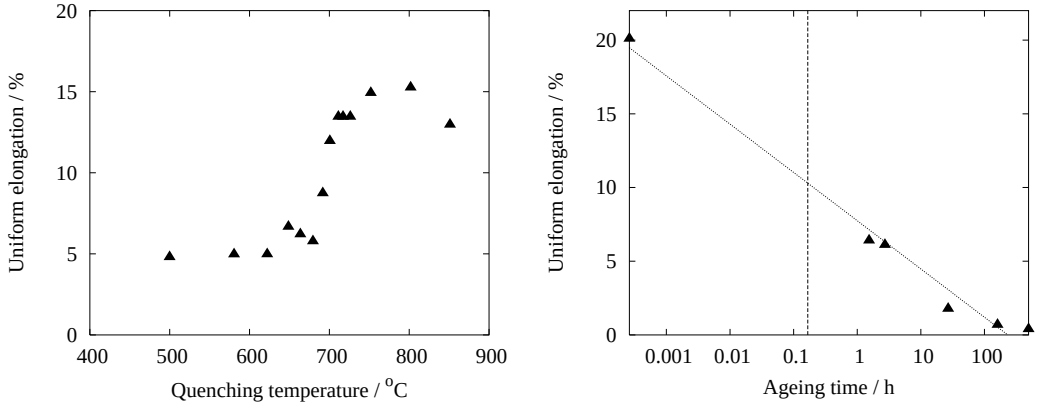

Figure 41: Uniform elongation at room temperature of Fe-48Co-2V samples quenched in iced brine after annealing 30 min at various temperatures, after [75].

Pitt and Rawlings [113] measured the ductility of a sample of Fe-49Co-2V (wt%) annealed 2.8 h at 850 °C then aged at 550 °C for different lengths of time. Their

results also indicate zero ductility after prolonged low-temperature treatment, in this case more than 100 h at 550 °C (while it is already zero after 10 h at 500 °C in the case of Zhao and Baker).

The hypothesis that vanadium prevents or delays the ordering reaction was quickly adopted following the discovery of its effect on ductility and is still quoted in relatively recent literature (for example [28, 81]). However, as noted by Stanley (1950, [117]), there is only circumstantial evidence.

As discussed in section 3.2.2, there is no clear indication that vanadium delays the ordering reaction, in fact some studies have pointed to an opposite trend. The results from Pitt and Rawlings [113] (figure 41) also cast doubts on the relationship order/brittleness as the ductility continues to decrease with ageing time well past the time expected to produce a fully ordered sample).

Indeed, Chen (1961, [17]) criticised early the idea that brittleness was entirely attributable to order. This author suggested that the ordering would add little to the brittleness inherent to b.c.c. structures, in particular when the alloy was not entirely free from interstitial atoms. From then, he proposed that the beneficial role of vanadium resided in its trapping the impurities and allowing a martensitic structure to be obtained after quenching.

These two suggestions have been later refuted. Kawahara [50] noted that, if the improvement of ductility due to vanadium additions is a result of its scavenging effect on impurities such as carbon, nitrogen and oxygen, one would expect the impact of the addition of different elements on ductility to scale with their affinity for these interstitials. However, Kawahara [50] observed no such correlation. As discussed later, Glezer and Maleyeva [116] have also established that the role of impurities was secondary.

The other factor put forward by Chen [17] as important in promoting low temperature ductility is the possibility to obtain a dual phase microstructure consisting of α and α'. Obtaining such a microstructure is made easier by additions of vanadium which open the high-temperature $\alpha + \gamma$ region, as discussed in section 2.2.1. However, it appears that vanadium also improves the ductility of alloys heat-treated in the single-phase α region [19]. Furthermore, as discussed in section 2.3.5, recent work on the addition of Nb have shown that, although Nb does not affect the width of the $\alpha + \gamma$ region, it nevertheless strongly promotes low-temperature ductility.

Kawahara [50], in turn, proposed an alternative mechanism by which ternary

additions improve ductility. He proposed that most additions that improve ductility do so through formation of Co_3X compounds such as γ_2 in FeCo-V. The precipitates, rich in cobalt, would be surrounded by a cobalt depleted zone which orders much more slowly if at all. These regions, assumed to be ductile, would impart ductility to the whole material. In addition to the fact that it is difficult to conceive how a few dispersed ductile region can impart ductility to the bulk material, the most important difficulty with Kawahara's suggestion is that such precipitates are usually not found [10] in the quenched state for FeCo-2V alloys, which are however ductile.

Intergranular and transgranular fracture An important impact of vanadium additions is that it suppresses intergranular fracture. Jordan and Stoloff [98], and Johnston *et al.* [99] reported transgranular cleavage in both ordered and disordered FeCo-2V alloys.

This has prompted investigations into the grain-boundary chemistry of FeCo and FeCo-2V. Glezer and Maleyeva [116] have compared the impurity segregation of FeCo and FeCo-2V after fracture, which was intergranular for the former and transgranular for the latter. However, opposite to the expected trend, they observed higher segregation of S, C and O in the FeCo-2V alloy, and therefore suggested that grain boundary disordering is a stronger factor in the suppression of intergranular brittleness.

If FeCo-2V is aged at high-temperature for more than 100 h, its ductility also drops to zero and intergranular failure is found to occur by a mixture of trans- and intergranular cleavage, the latter being attributed to the presence of large γ_2 particles on the grain boundaries.

It is possible to propose the following general view: in binary FeCo, failure always occurs through intergranular cleavage with 0% elongation, at stresses below that which would be required for transgranular cleavage or yield. The addition of vanadium suppresses intergranular embrittlement by a mechanism which is not confirmed, but probably relates to grain-boundary disordering. In this case, the material remains brittle in the ordered state, where fracture is controlled by transgranular cleavage, while is it ductile in the disordered state, as discussed later.

The implication of the grain boundary disordering hypothesis is that, whatever the apparent bulk order of the binary alloy, it is not possible to quench sufficiently fast to prevent grain boundary ordering. This would explain why intergranular

cleavage occurs in both ordered and 'disordered' samples. It must be noticed that, although most of the literature indicates intergranular failure in the binary alloy, ordered or disordered, the results of Marcinkowski and Larsen [115] show otherwise.

Although this provides a consistent view of the ductility, whether intergranular embrittlement is indeed related to grain boundary ordering remains to be directly proven. There is also no clear explanation as to the role of vanadium in preventing grain boundary embrittlement.

5.2.3 Effect of other additions

With the exception of additions of Ni, which has received significant attention [43, 43, 112, 113] for its beneficial effect on ductility, the impact of other elements has mostly been considered in terms of cold-rollability.

Influence of Ni additions As reported by Pitt and Rawlings [113] and Branson *et al.* [43], Ni additions improves significantly the ductility of FeCo-V alloys. This appear to be a consequence of the impact of Ni addition on γ_2 formation (discussed in section 2.2.3). This in turn results in significant grain refinement with typical grain size limited to 1.7 μm following heat-treatments producing grain sizes typically greater than 10 μm in FeCo-2V [113].

Other elements Orrock (1981 [19]), Kawahara (1983 [50]), and Major and Orrock (1988 [81]) investigated the effect of a number of addition to FeCo on its ductility following quench from high-temperature. Orrock [19], and Major and Orrock [81] reported the effect of Si, Cu, Ni, W, V, Nb and Ta on the cold workability of FeCo alloys quenched from 800 °C, and found that, while Nb, Ta and V were effective from 0.25, 0.2 and 2 at% respectively, the other additions were not (up to 5 at%).

The work of Kawahara [23] concerns a greater number of elements, but in different conditions, as the alloys were tested for cold workability following a heat-treatment at 1100 °C, in the γ region. Table 14 reproduces a few of the results from [23]; it is interesting to note that the impact of W and Mo appears to be strongly dependent on the exact stoichiometry of the alloy.

Unfortunately, Major and Orrock do not provide composition details for Fe and Co and it has been assumed, in table 14 that their results were for strictly equiatomic

compositions (a substantial amount of the literature so refers, however, to most compositions within 2% for equiatomic).

Composition (/ at%)			Cold rolling
Fe	Co	X	
49.75	49.75	0.5 W	no [81]
49.5	49.5	1.0 W	no [81]
49.25	49.25	1.5 W	no [81]
49.75	49.75	0.5 W	yes [23]
49.5	49.5	1.0 W	yes [23]
50	48	2 W	yes [23]
49	49	2 W	no [23]
49.5	49.5	1 Ni	no [81]
48.5	48.5	3 Ni	no [81]
47.5	47.5	5 Ni	yes [81]
49	49	2 Ni	no [23]
50	48	2 Ni	yes [23]

Table 14: Some of the results obtained by Kawahara [23] on the cold workability of FeCo-X alloys after quenching from 1100 °C, and Major and Orrock [81] after quenching from 800 °C.

Low carbon or boron additions were found to be inefficient in preventing intergranular fracture [50, 82], while larger additions of carbon (> 0.5 at%), or small additions B (0.16 at%) to FeCo-2V were found to allow cold-rolling [23] and enhance ductility [82] respectively.

5.2.4 Effect of temperature

Johnston *et al.* (1965 [99]) and later Jordan and Stoloff (1969, [98]) reported the temperature dependency on the ductility of FeCo-2V alloys. This is illustrated in figure 42, which shows that both the ordered and disordered state of the alloy present a ductile to brittle transition, however at vastly different temperatures.

As noted by Johnston *et al.* [99], the ordering reaction has an impact on the ductile-brittle transition temperature (DBTT) which is far greater than that of any other factor on conventional ferritic alloys (composition, grain-size, strain-rate), with

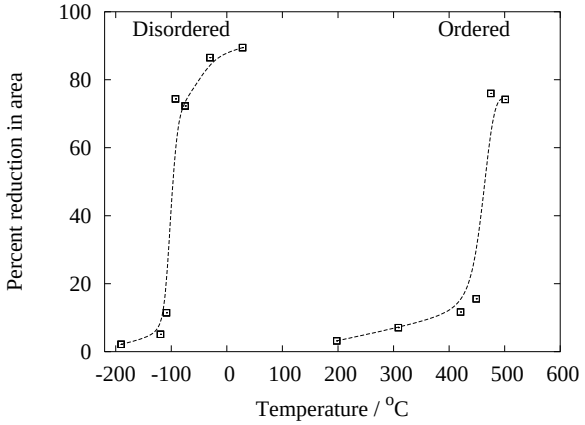

Figure 42: The ductility of ordered and disordered FeCo-2V as a function of temperature, after [99].

a shift close to 550 °C.

It has been reported earlier that a change in slip mode is observed from wavy to planar glide when the material orders [75, 98, 99], although there are disagreement as to which systems are active (section 5.1.1). Johnston *et al.* reported this change in both ordered and disordered material around the DBTT temperature. However, Jordan and Stoloff later [98] underlined the presence of both wavy and planar glide below and above the DBTT in the disordered material, while agreeing that the shift between ordered and disordered samples relates to a change in slip mode.

A similar change in ductility can be observed at room temperature if the alloy is quenched after heat-treatments inducing different degree of long-range order. This kind of experiments has already been discussed in section 5.1.1. Figure 41 illustrates the results obtained by Stoloff and Davies [75]. It must be noted that, although fully ordered, the sample annealed below $\sim$ 600 °C have a non-zero ductility.

5.2.5 Effect of grain size

Reducing the grain size, or in general the slip-distance, results in an increase of the DBTT (for example, [118]). The detrimental effect of grain growth on ductility is clearly illustrated in figure 41, where it is shown that ageing at 550 °C causes a reduction in ductility even past the time required to complete the ordering reaction. Over this time, the grain size increases from 37 to 80 μm [113]. Jordan and Stoloff also report a shift of the DBTT of both ordered and disordered FeCo-2V to higher

temperatures with decreasing grain sizes, but indicate that neither Cotrell-Petch fracture theory nor subsequent modifications appropriately describe the temperature dependence of the DBTT.

On the other side, as mentioned earlier, grain refinement by Ni addition (section 5.2.2) has lead to alloys equally ductile in the ordered and disordered state [113]. Similarly, grain refinement by low-temperature recrystallisation of FeCo-2V leads to sub-micron grain sizes and ductility similar to that of the disordered alloy [65]. While Pitt and Rawlings have reported a satisfying agreement with $\varepsilon_L \propto d^{-1/2}$, it is difficult to find support for this in other published data. Figure 43 presents the ductility of ordered FeCo-2V or FeCo-2V-Ni alloys of different grain sizes, it is clear that the trend is ill-defined.

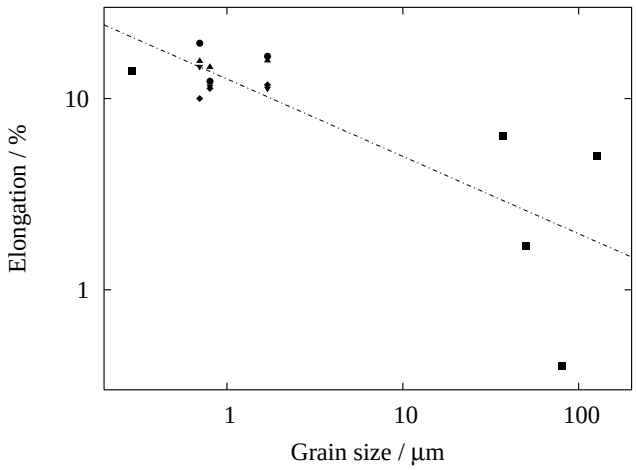

Figure 43: The ductility of FeCo-2V and FeCo2V-Ni alloys as a function of their grain size, using data from [65, 75, 113].

It has been suggested that incomplete recrystallisation results in lower ductility, so that a maximum is observed when the recrystallisation temperature is varied, as reported by Thornburg [59] for FeCo-2V and Hailer for FeCo-2V-Nb [93]. Figure 44 illustrates the influence of annealing temperature on the elongation, it is noticeable that the results from Duckham *et al.* [65] and those of Hailer [93], although obtained independently, fall in reasonable continuity. As discussed earlier (section 5.1.4) for strength, a comparison of independently measured grain size and predicted strength and coercivity indicates that the alloys studied by Thornburg [59] or Hailer [93] might have been fully recrystallised at temperature below T_c, where however grain

growth is particularly slow. In fact, Duckham *et al.* [65] suggest that recrystallisation is complete after 1 h at 650 °Cand 95% so after 1 h at 600 °C. A possible explanation for the incomplete recrystallisation reported by Thornburg or Hailer lies in the experimental techniques used, as it appears that only Duckham *et al.* have used Transmission Electron Microscopy (TEM) to characterise the amount of material recrystallised. Given the final grain sizes at low temperatures, this is likely to be the only suitable method. Assuming that samples are therefore fully recrystallised above 650 °C, it is not clear what causes the peak in ductility at intermediate grain sizes.

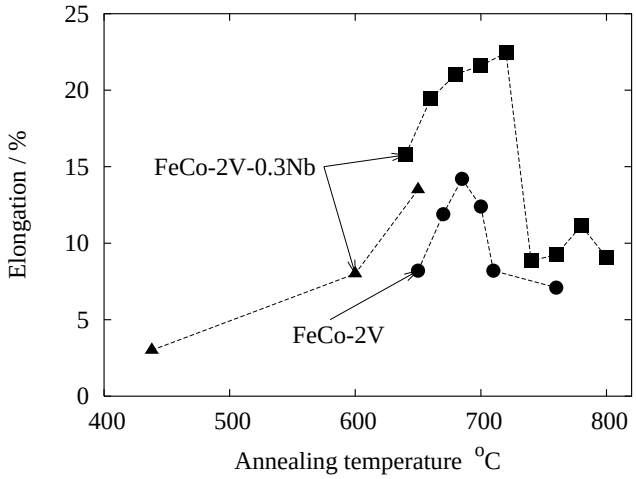

Figure 44: The ductility of FeCo-2V and FeCo-2V-0.3Nb alloys as a function of annealing temperature. All treatments 1 h for FeCo-2V-0.3Nb except at 438 °C (5 h), 2h for FeCo-2V. Lower temperature data for FeCo-2V-0.3Nb from [65], higher temperature from [93], data for FeCo-2V from [59].

6 Recent topics: high-temperature applications

This section, organised somewhat differently than the rest of this review, summarises areas which have received particular attention recently.

The FeCo alloys have recently been the object of renewed interest with the prospect of high temperatures applications [4]. Recent studies have underlined the shortcomings of existing materials and the present review highlights the need for further fundamental understanding.

6.1 Ageing of FeCo based alloys

A number of studies [34, 35, 71] have investigated the impact of long-term ageing at intermediate temperatures on the magnetic and mechanical properties, mostly of FeCo-V and FeCo-V-Nb alloys.

Zhu *et al.* [29] then Li *et al.* [34] reported changes in the magnetic properties in Hiperco 50 (FeCo-2V) during ageing at 450 °C. They observed a small increase in the degree of order, precipitation of a second-phase [29] together with a significant reduction of the permeability [34]. These different observations may be explained by the precipitation of γ_2: the formation of particles would have detrimental effects on the permeability, while the removal of vanadium from solid solution would allow the small increase of order (as discussed earlier in section 3.2.2, vanadium reduces the maximum degree of long range order).

However, this is difficult to conciliate with previous results (section 2.2.2) which show that γ_2 would not be expected before about 1000 h at this temperature, while the changes reported above occur essentially within the first 200 h of ageing. Furthermore, the authors [29] report a primitive cubic lattice with lattice parameter 2.82 Å, which is not the structure expected for γ_2.

The modern variants of FeCo-2V studied above (Hiperco H50) contains small additions of Nb (0.03 wt%) which refine the grain size. The compositions studied by Ashby *et al.* [10] or in similar studies (up to late 1970s) would not contain such addition. It is therefore possible that the formation of γ_2 is accelerated in recent alloys, either by the grain size refinement (increase in heterogeneous nucleation sites) or via a direct stabilisation of γ_2 by Nb. That Nb additions promotes γ_2 precipitation is further supported by the evolution of the resistivity in H50 (FeCo-2V) and H50HS (FeCo-2V-0.3Nb). Geist *et al.* [35] followed the evolution of resistivity for H50 and

H50HS during ageing at 550 °C, after annealing 90 min at 720 °C and slow cooling to room temperature. As illustrated in figure 45, the resistivity of H50 decreases steadily over the first 1000 h. This may correlate with γ_2 precipitation which removes vanadium from solid solution [119], although in such case, the resistivity has been shown to increase first, possibly because of lattice strain [119,120]. This may not be visible because of the time scale of the investigation, or because precipitation has already started during the slow cooling. In H50HS, there is no significant change in resistivity, which may indicate that the annealing treatment and/or the slow cool were sufficient to precipitate most of the vanadium. In fact, Shang *et al.* have reported the presence of second phases in both H50 and H50HS in similar conditions [33].

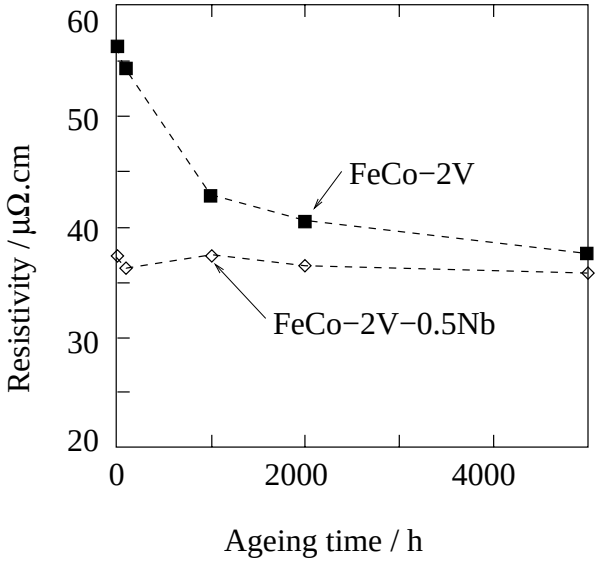

Figure 45: The resistivity of H50 and H50HS as a function of ageing at 550 °C, after [35].

Regrettably, the evolution of the resistivity, coercivity and losses during ageing [34,35,71] was not supported by a microstructural investigation.

6.2 Creep

The creep resistance of FeCo alloys has been investigated by Fingers [121,122]. This investigation essentially covers high stresses between 275 and about 900 MPa. While different behaviours are observed, there is no attempt to identify creep mechanisms

of link these differences with microstructural changes.

Yu *et al.* [31] produced tungsten fibres reinforced FeCo alloy and obtained significant improvement in the creep strength, however the tests were also limited to about 100 h. The present author is not aware of continuation of this work.

7 Summary

The current state of knowledge regarding the constitution of near equiatomic FeCo based alloys has been reviewed, together with their mechanical and magnetic properties.

The Constitution and thermodynamics of the binary alloy now appear satisfyingly described, although recent work such as [14] still challenge most of the current knowledge. Most studies concerning the effect of alternative additions have been undertaken in the 30s. With exception of vanadium and other topical contributions, little progress has been made since. In particular, there has been no attempt to reconcile the observation of ordered γ_2 phases with typical isopleth sections which show corresponding bulk composition in the $\alpha + \gamma$ field. The interaction between V, Nb and Ta remains to study. The ordering reaction is rather well characterised for binary alloys, but as above, difficulties subsist in other systems. Although a good part of the literature indicates that vanadium has no influence on the ordering kinetics, relatively recent work on the problem do not necessarily agree, as in the case of Orrock [19].

The strength and ductility of FeCo based alloys exhibit peculiarities that are not necessarily found in other B2 structures such as FeAl. In particular, a maximum occurring near the critical temperature for ordering is still not satisfyingly explained. This review underlines the importance of grain size in determining the strength at a given temperature, in many cases, second-phase particles mainly contribute by controlling the grain size. As for ductility, it seems well established that the low ductility of the binary alloy are attributable to a grain boundary embrittlement, as this alloy is most often observed to fracture intergranularly in both ordered and disordered conditions. The role of vanadium in promoting ductility in samples quenched from high temperatures seems to be related to its suppressing the grain boundary embrittlement. The ordered state remains brittle due to the limited numbers of slip systems, however this time failing mainly by intragranular fracture, and

with detectable deformation ($\sim$ 4-5%). Other elements have been found that have the same influence on ductility, such as Nb or Ta. The only explanation that has been put forward for their effect is the same as that initially proposed for vanadium, and later refuted, whereby the addition is thought to slow the ordering kinetics.

The coercivity is strongly dependent on the microstructural features, which in most commercial alloys is limited to grain boundaries. It has been shown that various results from independent studies on different FeCo based alloys exhibited a coercivity that is virtually only dependent on the grain size. The problem is more complex when precipitates are present, as it is clear that their influence on the coercivity cannot be rationalised without more detailed information than usually published (size distribution, location). The saturation is little dependent on the microstructure. In some cases, such as FeCo-Nb and FeCo-Ta, saturations have been reported in excess of that expected at the peak corresponding to Fe-0.35Co.

8 Acknowledgements

The author is grateful to EPSRC and Rolls-Royce, in particular S. W. Hill, for funding the project this work is part of and for useful comments, and to Pr. H. K. D. H. Bhadeshia for support and discussions.

References

[1] McHenry M. E., Willard M. A., and Laughlin D. E. Amorphous and nanocrystalline materials for applications as soft magnets. *Prog. Mater. Sci.*, 44:291–433, 1999.

[2] G. W. Elmen. Magnetic material and appliance. US patent No 1,739,752, 1929.

[3] J. H. White and C. V. Wahl. Workable magnetic compositions containing principally iron and cobalt. US patent No 1,862,559, 1932.

[4] R. T. Fingers and C. S. Rubertus. Application of high temperature magnetic materials. *IEEE Trans. Magnetics*, 36:3373–3375, 2000.

[5] T. Nishizawa and K. Ishida. *Binary alloy phase diagrams*, volume 2. ASM International, OH, 2nd edition, 1990.

[6] I. Ohnuma, H. Enoki, O. Ikeda, R. Kainuma, H. Ohtani, B. Sundman, and K. Ishida. Phase equilibria in the Fe-Co binary system. *Acta Mater.*, 50:379–393, 2002.

[7] J. E. Bennett and M. R. Pinnel. Aspects of phase equilibria in Fe-Co 2.5 to 3.0% V alloys. *J. Mater. Sci*, 9:1083–1090, 1974.

[8] S. Mahajan, M. R. Pinnel, and J. E. Bennett. Influence of heat treatments on microstructures in an Fe-Co-V alloy. *Metall. Trans.*, 5:1263–1272, 1974.

[9] M. R. Pinnel and J. E. Bennett. Correlation of magnetic and mechanical properties with microstructure in Fe-Co-2-3V alloys. *Metall. Trans.*, 5:1273–1283, 1974.

[10] J. A. Ashby, H. M. Flower, and R. D. Rawlings. Gamma phase in an Fe-Co-2%V alloy. *Metal Sci*, 11:91–96, 1977.

[11] W. C. Ellis and E. S. Greiner. Equilibrium relations in the solid state of the iron-cobalt system. *Trans. ASM*, pages 415–433, 1941.

[12] A. S. Normanton, P. E. Bloomfield, F. R. Sale, and B. B. Argent. A calorimetric study of iron-cobalt alloys. *Metal Sci.*, 9:510–517, 1975.

[13] Z. Turgut, J. H. Scott, Q. Huang, S. A. Majetich, and M. E. Mc-Henry. Magnetic properties and ordering of C-coated Fe_xCo_{1-x} alloy nanocrystals. *J. Appl. Phys.*, 83:6468–6470, 1998.

[14] Y. Ustinovshikov and S. Tresheva. Character of transformations in Fe-Co system. *Mat. Sci. Eng. A*, A248:238–244, 1998.

[15] R. W. Fountain F. Libsch. Development of mechanical and magnetic hardness in a 10% v-co-fe alloy. *Trans. AIME*, 197:349–356, 1953.

[16] D. L. Martin and A. H. Geisler. Constitution and properties of cobalt-iron-vanadium alloys. *Trans. ASM*, 44:461–483, 1952.

[17] C. W. Chen. Metallurgy and Magnetic Properties of an Fe-Co-V alloy. *J. Appl. Phys.*, 32(3):348S–355S, 1961.

[18] C. D. Pitt and R. D. Rawlings. Microstructure of Fe-Co-2V and Fe-Co-V-Ni alloys containing 1.8-7.4 wt% Ni. *Metal Sci.*, 15:369–376, 1981.

[19] C. M. Orrock. *PhD thesis*. PhD thesis, London University, 1986.

[20] National Physical Laboratory, Teddington, Middlesex, UK. *MT-DATA Handbook, Utility Module*.

[21] W. Koster and H. Schmidt. Das Dreistoffsystem Eisen-Kobalt-Vanadin. Teil I: ausbildung des dreistoffsystems bei gehemmter α/γ-Umwandlung. *Arch. Eisenhutten.*, 26:345–353, 1955.

[22] W. Koster and H. Schmidt. Das Dreistoffsystem Eisen-Kobalt-Vanadin. Teil II: die ausbildung des dreistoffsystems bei gleichgewicht zwischen α/γ-Mischkristallen. *Arch. Eisenhutten.*, 26:421–425, 1955.

[23] K. Kawahara. Structures and mechanical properties of an FeCo-2V alloy. *J. Mat. Sci.*, 18:3427–3436, 1983.

[24] A. I. C. Persiano and R. D. Rawlings. Effect of niobium additions on the structure and magnetic properties of equiatomic iron-cobalt alloys. *J. Mat. Sci.*, 26:4026–4032, 1991.

[25] Fiedler H. C. and Davis A. M. The formation of gamma phase in vanadium permendur. *Metall. Trans.*, 1:1036–1037, 1970.

[26] S. Mahajan and K. M. Olsen. An electron microscopic study of the origin of coercivity in an fe-co-v alloy. In *Magnetism and Magnetic Materials, 20th Conf. San Francisco*, pages 743–744, 1974.

[27] K. Kawahara. Effect of cold rolling on the mechanical properties of an FeCo-2V alloy. *J. Mat. Sci.*, 18:3437–3448, 1983.

[28] A. I. C. Persiano and R. D. Rawlings. Effects on some physical properties of soft magnetic Fe-Co alloys due to the replacement of vanadium by niobium. *J. Mater. Eng.*, 12:21–27, 1990.

[29] Q. Zhu, L. Li, M. S. Masteller, and G. J. Del Corso. An increase of structural order parameter in Fe-Co-V soft magnetic alloy after thermal aging. *Appl. Phys. Lett.*, 69(25):3917–3919, 1996.

[30] P. M. Novotny. The effect of nickel content on the ac magnetic properties of 49Fe-49Co-2V alloys. *J. Appl. Phys.*, 63(8):2977–2979, 1988.

[31] R. H. Yu, S. Basu, R. Y. Zhang, A. Parvizi-Marjidi, K. M. Unruh, and J. Q. Xiao. High temperature soft magnetic materials: FeCo alloys and composites. *IEEE Trans. Magn.*, 36(5):3388–3393, 2000.

[32] R. H. Yu, S. Basu, Y. Zhang, and J. Q. Xiao. Magnetic domains and coercivity in FeCo soft magnetic alloys. *J. Appl. Phys.*, 85(8):6034–6036, 1999.

[33] C. H. Shang, R. C. Cammarata, T. P. Weihs, and C. L. Chien. Microstructure and Hall-Petch behavior of Fe-Co based Hiperco alloys. *J. Mater. Res.*, 15(4):835–837, 2000.

[34] R. T. Fingers, R. P. Carr, and Z. Turgut. Effect of aging on magnetic properties of Hiperco 27, Hiperco 50 and Hiperco 50HS. *J. Appl. Phys.*, 91(10):7848–7850, 2002.

[35] B. Geist, T. Peterson, J. C. Horwath, Z. Turgut, M. Q. Huang, R. A. Snyder, and R. T. Fingers. Effect of high-temperature aging on electrical properties of Hiperco 27, Hiperco 50 and Hiperco 50HS. *J. Appl. Phys.*, 93(10):6686–6688, 2003.

[36] T. Sourmail. Precipitation in creep resistant austenitic stainless steels. *Mater. Sci. Tech.*, 17:1–14, 2001.

[37] W. Köster and W. Tonn. Das system eisen-kobalt-wolfram. *Arch. Eisenhutten.*, 5:431–440, 1932.

[38] W. Köster and W. Tonn. Das system eisen-kobalt-molybdän. *Arch. Eisenhutten.*, 5:627–620, 1932.

[39] W. Köster and W. Schmidt. Das system eisen-kobalt-mangan. *Arch. Eisenhutten.*, 7:121–126, 1933.

[40] W. Köster and W. Schmidt. Eigenschaftänderungen irreversibler ternärer eisenlegierungen durch wärmebehandlung. *Arch. Eisenhutten.*, 8:491–498, 1935.

[41] M. Dombre, O. S. Campos, N. Valignat, C. Allibert, C. Bernard, and J. Driole. Solid state phase equilibrium in the ternary fe-co-cr system: experimental determination of isothermal sections in the temperature range 800-1300 c. *J. Less Common Metals*, 66:1–11, 1979.

[42] B. Thomas. The influence of nickel on the magnetic and mechanical properties of co-fe-v alloy. *IEEE Trans. Magn.*, 16:444–454, 1980.

[43] M. W. Branson, R. V. Major, C. Pitt, and R. D. Rawlings. A study of the microstructure and related magnetic/mechanical properties of some iron-cobalt-vanadium and iron-cobalt-vanadium-nickel alloys. *J. Magn. Magn. Mater.*, 19:222–224, 1980.

[44] W. Köster. Das system eisen-kobalt-chrom. *Arch. Eisenhutten.*, 6:113–116, 1932.

[45] W. Koster and Hofmann G. Uber die instellung im dreistoffsystem eisen-kobalt-chrom. *Arch. Eisenhutt.*, 30:249–251, 1959.

[46] V. G. Rivlin. Critical evaluation of constitution of cobalt-chromium-iron and cobal-iron-nickel systems. *Int. Met. Rev.*, 5:269–300, 1981.

[47] W. Koster and W. D. Haehl. Zustandsanderungen bei der warmebahandlung von eisen-kobalt-nickel-legierungen mit nickelgehalten bis 40% und ihr einfluss auf die eigenschaften der legierungen. *Arch. Eisenhutt.*, 40:575–583, 1969.

[48] S. Widge and J. I. Goldstein. Redetermination of the fe-rich portion of the fe-ni-co phase diagram. *Metall. Trans. A*, 8:309–315, 1977.

[49] W. Koster and M. Speidel. Uber die gleichgewichtseinstellung im dreistoffsystem eisen-kobalt-mangan. *Arch. Eisenhutt.*, 33:873–876, 1962.

[50] K. Kawahara. Effect of additive elements on cold workability of FeCo alloys. *J. Mat. Sci.*, 18:1709–1718, 1983.

[51] W. Köster. Mechanische und magnetische ausscheidungshärtung der eisen-kobalt-wolfram und eisen-cobalt-molybdän-legierungen. *Arch. Eisenhutten.*, 6:17–23, 1932.

[52] M. F. S. Rezende, Mansur R. A., Pfannes H. D., and Persiano A. I. C. Phase chracterization in the Fe-Co-V and Fe-Co-Nb systems. *Hyperfine Interactions*, 66:319–324, 1991.

[53] A. J. Griest, Libsch J. F., and G. P. Conard. Effect of ternary additions of silicon and aluminium on the ordering reaction in iron-cobalt. *Acta Metall.*, 3:509–510, 1955.

[54] M. M. Borodkina, E. I. Detalf, and Y. P. Selisskiy. Recovery and recrystallisation of ordering alloys. Fe-Co. *Fiz. Metal. Metalloved.*, 7:214–224, 1959.

[55] Y. P. Selliskiy and M. N. Tolochko. The problem of recrystallisation of ordering alloys of iron and cobalt. *Fiz. Metal. Metalloved.*, 13(4):587–590, 1962.

[56] A. A. Goldenberg and Y. P. Selliskiy. Recrystallisation parameters and ordering effect in alloys on the system fe-co. *Fiz. Metal. Metalloved.*, 15(5):717–724, 1963.

[57] Davies R. G. and Stoloff N. S. A study of grain growth in feco-v. *Trans. Met. Soc. AIME*, 236:1605–1608, 1966.

[58] L. Ren, S. Basu, R. H. Yu, J. Q. Xiao, and A. Parvizi-Majidi. Mechanical properties of Fe-Co soft magnets. *J. Mater. Sci.*, 36:1451–1457, 2001.

[59] D. R. Thornburg. High-strength high-ductility cobalt-iron alloys. *J. Appl. Phys.*, 40:1579–1580, 1969.

[60] F. J. Humphreys and Hatherly. *Recrystallisation and Related Phenomena.* Pergamond, Elsevier Science, Oxford, U.K., 1996.

[61] T. Sourmail. Evolution of strength and coercivity during annealing of FeCo based alloys. *Scripta Mater.*, 51:589–591, 2004.

[62] X. M. Cheng, X. K. Zhang, D. Z. Zhang, S. H. Lee, A. Duckham, T. P. Weihs, R. C. Cammarata, J. Q. Xiao, and C. L. Chien. Magnetic core loss of ultrahigh strength FeCo alloys. *J. Appl. Phys.*, 93(10):7121–7123, 2003.

[63] R. A. Buckley. Ordering and recrystallisation in Fe-50Co-0.4%Cr. *Metal Sci.*, 13:67–72, 1979.

[64] R. A. Buckley. Microstructure and kinetics of the ordering transformation in iron-cobalt alloys, FeCo, FeCo-0.4%Cr, FeCo-2.5%V. *Metal Sci*, 19:243–247, 1975.

[65] A. Duckham, D. Z. Zhang, D. Liang, V. Luzin, R. C. Cammarata, C. L. Leheny, C. L. Chien, and T. P. Weihs. Temperature dependent mechanical properties of ultra-fine grained FeCo-2V. *Acta Mater.*, 51:4083–4093, 2003.

[66] R. H. Yu, S. Basu, Y. Zhang, A. Parvizi-Majidi, and J. Q. Xiao. Pinning effect of the grain boundaries on magnetic domain wall in FeCo-based magnetic alloys. *J. Appl. Phys.*, 85(9):6655–6659, 1999.

[67] C. W. Chen. *Magnetism and metallurgy of soft magnetic materials*. North-Holland Publishing Company, Amsterdam, 1977.

[68] D. W. Clegg and R. A. Buckley. The disorder-order transformation in iron-cobalt-based alloys. *Metal Sci. J.*, 7:48–54, 1973.

[69] A. W. Smith and R. D. Rawlings. A neutron diffraction study of ordering in an iron-cobalt-1.8% vanadium alloy. *Phys. Stat. Sol. A*, 34:117–123, 1976.

[70] C. G. Shull and S. Siegel. Neutron diffraction studies of order-disorder in alloys. *Phys. Rev.*, 75:1008–1010, 1949.

[71] L. Li. High temperature magnetic properties of 49%Co-2%V-Fe alloy. *J. Appl. Phys.*, 79(8):4578–4580, 1996.

[72] J. E. Goldman and R. Smoluchowski. Influence of order on the saturation magnetic moment. *Phys. Rev.*, 75:310–311, 1949.

[73] L. Kussmann. volume 13. 1932.

[74] J. W. Rodgers and W. R. Maddocks. The influence of the alloying element on the ae3 point in iron-cobalt and other alloys. Technical report, Second alloy steels report-Section VIII, 1939.

[75] N. S. Stoloff and R. G. Davies. The platic deformation of ordered FeCo and Fe_3Al alloys. *Acta Metall.*, 12:473–485, 1964.

[76] P. Grosbras, J. P. Eymery, and P. Moine. Nature de la transformation desordre-ordre dans les alliages fer-cobalt. Influence de l'addition de vanadium. *Acta Metall.*, 24:189–196, 1976.

[77] M. Rajkovic and R. A. Buckley. Ordering transformations in fe-50co based alloys. *Metal Sci.*, pages 21–29, 1981.

[78] P. Grosbras, J. P. Eymery, and P. Moine. Cinétiques d'établissement de l'ordre dans un alliage fe-co-v écroui. *Scripta Metall.*, 7, 1973.

[79] J. K. Stanley. Metallurgical factors affecting the magnetic and mechanical properties of iron-cobalt alloys. *Trans. A.S.M.*, 42:150–174, 1950.

[80] J. P. Eymery, P. Grosbras, and P. Moine. Ordering kinetics of various Fe-Co alloys. *Phys. Stat. Sol. A*, 21:517–528, 1974.

[81] R. V. Major and C. M. Orrock. High saturation ternary cobal-iron based alloys. *IEEE Trans. Magn.*, 24:1856–1858, 1988.

[82] E. P. George, A. N. Gubbi, I. Baker, and L. Robertson. Mechanical properties of soft magnetic feco alloys. *Mater. Sci. Eng. A*, 329-331:325–333, 2002.

[83] A. T. English. Long range ordering and domain-coalescence kinetics in fe-co-2v. *Trans. Met. Soc. AIME*, 236:14–18, 1966.

[84] J. A. Rogers, H. M. Flower, and R. D. Rawlings. The electron metallography of antiphase domain growth in FeCo-2%V. *Metal Sci.*, 9:32–35, 1975.

[85] J. F. Dinhut, H. Garem, J. P. Eymery, and P. Moine. Thermal ordered domains and mechanical antiphase boundaries as studied by electron microscopy in fe-co-v. *Scripta Metall.*, 8:307–312, 1974.

[86] T. Sourmail. Comments on 'Character of transformations in Fe-Co system'. *Scripta Mater.*, in press, 2005.

[87] M. F. Collins and J. B. Forsyth. The magnetic moment distribution in some transition metal alloys. *Phil. Mag.*, 8:401–410, 1963.

[88] C. Kuhrt and L. Schultz. Formation and magnetic properties of nanocrystalline mechanically alloyed Fe-Co and Fe-Ni. *J. Appl. Phys.*, 73:6588–6590, 1993.

[89] B. V. Reddy amd S. C. Deevi and S. N. Khanna. Magnetic properties of Al, V, Mn and Ru impurities in Fe-Co alloys. *J. Appl. Phys.*, 93(5):2823–2827, 2003.

[90] R. T. Fingers and G. Kozlowski. Microstructure and magnetic properties of Fe-Co alloys. *J. Appl. Phys.*, 81(8):4110–4111, 1997.

[91] L. Zhao and I. Baker. The effect of grain size and Fe:Co ratio on the room temperature yielding of FeCo. *Acta Metall. Mater.*, 42(6):1953–1958, 1994.

[92] D. A. Porter and K. E. Easterling. *Phase Transformations in Metals and Alloys*. Chapmann and Hall, London, 2 edition, 1992.

[93] B. T. Hailer. Effect of heat treatment on magnetic and mechanical properties of iron-cobalt-vanadium-niobium alloy. Master's thesis, Virginia Polytechnic Institute, Blacksburg, Virginia, 2001.

[94] G. K. Simon, R. E. Perrin, M. C. Ohmer, and T. L. Peterson. Resistivity of fecota high strength laminates from -73 c to 650 c. Technical Report WL-TR-97-4047, Whright Laboratory, Wright-Patterson Air Force Base, Ohio, 1997. available on http://stinet.dtic.mil.

[95] M. J. Marcinkowski. The effect of atomic order on the mechanical properties of alloys with emphasis on feco. In H. Warlimont, editor, *Order-disorder transformations in alloys*, pages 364–403, Berlin, 1974. Springer-Verlag.

[96] M. J. Marcinkowski and H. Chessin. Relationship between flow stress and atomic order in the feco alloy. *Phil. Mag.*, 10:837–859, 1964.

[97] P. Moine, J. P. Eymery, and P. Grosbras. The effects of short-range order and long-range order on the equilibrium configuration of superdislocations in fe-co-2at%v - consequences on flow stress. *Phys. Stat. Sol. B*, 46:177–185, 1971.

[98] K. R. Jordan and N. S. Stoloff. Plastic deformation and fracture in FeCo-2%V. *Trans. Metal. Soc. AIME*, 245:2027–2034, 1969.

[99] T. L. Johnston, R. G. Davies, and N. S. Stoloff. Slip character and the ductile to brittle transition of single-phase solids. *Phil. Mag.*, 12:305–317, 1965.

[100] M. Yamagushi, Y. Umakoshi, T. Yamane, Y. Minonishi, and S. Morozumi. Slip systems in an fe-54% co alloy. *Scripta Mater.*, 16:607–609, 1982.

[101] R. Carleton, E. P. George, and R. H. Zee. Effect of deviations from stoichiometry on the strength anomaly and fracture behaviour of b-doped feal. *Intermetallics*, 3:433–441, 1995.

[102] D. G. Morris. The yield stress anomaly in fe-al alloys: the local climb lock model. *Phil. Mag.*, 71:1281–1294, 1995.

[103] K. Yoshimi, S. Hanada, and M. H. Yoo. Yield stress anomaly in b2 feal. In C. C. Koch, C. T. Liu, N. S. Stoloff, and A. Wanner, editors, *High-Temperature ordered intermetallics alloys VII*, volume 460, pages 313–324, Boston, 1997. MRS, Materials Research Society.

[104] L. M. Pike, Y. A. Chang, and C. T. Liu. Point defect concentrations and hardening in binary b2 intermetallics. *Acta Mater.*, 45:3709–3719, 1997.

[105] H. Xiao and I. Baker. The temperature dependence of the flow and fracture of fe-40al. *Scripta Metall. Mater.*, 28:1411–1416, 1993.

[106] E. P. George and I. Baker. A model for the yield strength anomaly in feal. *Phil. Mag. A*, 77:737–750, 1998.

[107] I. Baker and E. P. George. A model for the yield strength anomaly in feal. In C. C. Koch, C. T. Liu, N. S. Stoloff, and A. Wanner, editors, *High-Temperature ordered intermetallics alloys VII*, volume 460, pages 373–378, Boston, 1997. MRS, Materials Research Society.

[108] Y. Yang, I. Baker, G. T. Gray, and C. Cady. The yield stress anomaly in stoichiometric feal at high strain rate. *Scripta Mater.*, 40:403–408, 1999.

[109] E. P. George and I. Baker. Thermal vacancies and the yield anomaly of feal. *Intermetallics*, 6:759–763, 1998.

[110] I. Baker and Y. Yang. On the yield stress anomaly in stoichiometric feal. *Mater. Sci. Eng. A*, 239-240:109–117, 1997.

[111] M. Kupka. Temperature dependence of the yield stress of an feal base alloy. *Mater. Sci. Eng. A*, 336:320–322, 2002.

[112] C. D. Pitt. *PhD thesis*. PhD thesis, London University, 1981.

[113] C. D. Pitt and R. D. Rawlings. Lüders strain and ductility of ordered Fe-Co-2V and Fe-Co-V-Ni alloys. *Metal Sci.*, 17:261–266, 1983.

[114] V. Bata and E. V. Pereloma. An alternative physical explanation of the hall-petch relation. *Acta Mater.*, 52:657–665, 2004.

[115] M. J. Marcinkowski and J. Larsen. The effect of atomic order on fracture surface morphology. *Metall. Trans.*, 1:1034–1036, 1970.

[116] A. M. Glezer and I. V. Maleyeva. Grain boundary fracture of ordered alloy feco. *Phys. Met. Metall.*, 66(6):174–176, 1988.

[117] M. F. S. Rezende, Mansur R. A., Pfannes H. D., Persiano A. I. C., Ardisson J. D., and Persiano A. I. C. Gamma to alpha phase transformation in FeCoV alloys. *Hyperfine Interactions*, 83:231–234, 1994.

[118] G. E. Dieter. *Mechanical Metallurgy*. Mc Graw Hill, London, 3 edition, 1988.

[119] J. A. Ashby, H. M. Flower, and R. D. Rawlings. Correlation of electrical resistivity with microstructure in an fe-co-2%v alloy. *Phys. Stat. Sol. A*, 47:407–414, 1978.

[120] D. M. Dzhavadov and Y. P. Selisskiy. Regularities in the variation of electrical resistivity of low-alloy iron-cobalt alpha-solid solutions as a result of heat-treatment. I: FeCo alloyed with vanadium. *Fiz. Metal. Metalloved.*, 15:504–510, 1963.

[121] Fingers R. T. *Creep behavior of thin laminates or iron-cobalt alloys for use in switched reluctance motors and generators*. PhD thesis, Virginia Polytechnic Institute, 1998.

[122] R. T. Fingers, J. E. Coates, and N. E. Dowling. Creep Deformation of a soft magnetic iron-cobalt alloy. *J. Appl. Phys.*, 85(8):6037–6039, 1999.